with IM11 (forward, 5′-TTC CAC TAC GTG ACG GGC AT-3′) and 5OA2KI (reverse, 5′-CCC GTC CAT GTG TAG GAC AT-3′). After denaturation at 98°C for 30 s, 35 cycles of amplification were set as follows: denaturation for 10 s at 98°C, annealing of primers for 30 s at 66°C, and extension for 15 s at 72°C, followed by final extension at 72°C for 5 min. The amplified PCR products were separated on a 2% agarose gel and purified by GENECLEAN II kit (Q-Bio Gene, Carlsbad, CA). Nucleotide sequences were determined using Big Dye Deoxy Terminator Cycle Sequencing kit (Perkin-Elmer, Tokyo, Japan). Nucleotide and aa sequences were compared with the nucleotide sequences of genotype 1b HCV-J (Gene Bank accession number; D90208) [22].

Statistical analysis

Variables between the SVR and non-SVR groups were compared using non-parametric tests (Mann–Whitney *U* test, two-tailed test and Fisher's exact probability test). Analyses for efficacy and safety were conducted on an intention-to-treat (ITT) basis, performed on patients who received at least one dose of the study medication.

Predictors of SVR were determined using univariate analyses. All p values <0.05 by two-tailed tests were considered significant. Potential predictive factors associated with SVR included sex, age, body mass index (BMI), viremia level, number of mutations in the ISDR, HCV core region (double mutant/non-double mutant), time from transplantation to therapy, duration of treatment, adherence to PEGIFN treatment, and adherence to RBV and EVR treatment. Statistical analyses were performed using the SPSS software (SPSS Inc., Chicago, IL).

Results

Patients characteristics

Table I shows the baseline characteristics of the 27 patients with recurrent hepatitis C after LT who were treated with PEGIFN/RBV combination therapy. The median age of patients was 56 years, and 17 were male. Median body mass index was 24.3. Most patients were infected with HCV genotype 1 ($n = 24$) and genotype 2 ($n = 3$). Median time for the initiation of antiviral therapy after transplantation was 4 months, and median pretreatment serum HCV RNA levels were 6.6 log IU/ml. Immunosuppressive therapy included tacrolimus in 22 of 27 patients, and cyclosporine in 5 of 27.

Table I. Characteristics of 27 patients with recurrent hepatitis C after living donor liver transplantation.

Age (years)*	56 (29–69)
Gender (male/female)	17/10
Body mass index*	24.3 (14.8–42.2)
Genotype (1/2)	24/3
Viral load at therapy (log IU/ml)*	6.6 (4.9–7.8)
Time from transplantation to therapy (months)*	4 (1–41)
Immunosuppression (tacrolimus/cyclosporine)	22/5

*Values are median (range).

Efficacy and safety assessment

Among 27 patients who were treated with antiviral therapy, 17 were able to complete our protocol (15 patients with genotype 1, 2 patients with genotype 2), whereas 10 patients had to discontinue the protocol (9 patients with genotype 1, 1 patient with genotype 2). SVR rate with PEGIFN/RBV was 37.0% (10/27). By genotype, SVR rate in patients with genotype 1 was 29.2% (7/24) and 100% (3/3) in those with genotype 2 (Figure 1). Most patients with genotype 1b whose HCV RNA reached undetectable level achieved SVR, at 87.5% (7/8), with only one patient not achieving SVR (Table II) (Figure 2).

Ten patients discontinued treatment, due to liver failure owing to the recurrence of HCV in 5 patients, general fatigue in 2, ALT flare due to acute rejection in 1 patient, anemia in 1, and depression in 1 (Figure 1).

Efficacy of long-term interferon therapy for genotype 1b patients

Table II shows details of patients who were treated with PEGIFN/RBV until HCVRNA had reached undetectable levels and were then further treated for at least more than 1 year.

Seven patients achieved SVR by prolonged PEGIFN/RBV for at least 1 year or more. Seven patients were male.

Eight patients had reached undetectable levels of HCV RNA and 7 patients had never reached undetectable levels of HCV RNA. Although 5 of the 8 patients were classified as LVR, 4 patients of these 5 achieved SVR. One male patient aged 69 years (patient no. 5) who had double mutation of aa 70 and aa 91 in the core region and zero substitutions in ISDR achieved SVR after prolongation of therapy (Figure 3). By contrast, another male aged 51 years (patient no. 9) who had double wild aa 70 and aa 91 in the core region and five substitutions in the ISDR did not achieve SVR after prolongation of therapy (Figure 4).

Table II. Details of 15 patients (genotype 1).

Patient no.	Age (years)	Gender	HCV RNA (log IU/ml)	HCV core region (aa 70/aa 91)	Number of mutations in the ISDR	Time from transplantation to therapy (months)	Time to reach undetectable levels of HCV RNA (weeks)	Treatment duration of VR (weeks)	Treatment duration (weeks)	Adherence to PEGIFN (%)	Adherence to RBV (%)	SVR
1	63	Male	6.1	m/m	4	41	3	103	106	35	29	Yes
2	60	Male	5.8	w/w	1	13	10	48	58	100	62	Yes
3	66	Male	6.6	m/m	3	12	12	60	72	80	11	Yes
4	54	Male	6.5	w/w	3	4	16	56	72	77	54	Yes
5	69	Male	6.3	m/m	0	12	21	57	78	42	14	Yes
6	44	Male	6.6	w/m	0	1	28	76	104	88	47	Yes
7	53	Male	6.1	m/w	1	2	54	125	179	57	25	Yes
8	56	Male	6.6	m/w	0	2	27	52	79	66	7	No
9	51	Male	5.9	w/w	5	6	NR	NR	173	80	25	No
10	47	Female	6.6	m/m	1	3	NR	NR	124	63	15	No
11	59	Female	6.6	m/w	1	7	NR	NR	86	100	65	No
12	64	Female	5	m/m	0	3	NR	NR	81	72	25	No
13	58	Female	6.6	m/m	1	3	NR	NR	79	83	63	No
14	65	Female	5.9	w/m	0	3	NR	NR	79	45	19	No
15	56	Male	7.2	m/w	0	3	NR	NR	58	51	26	No

Abbreviations: m = mutant; w = wild; NR = non-virological responder; VR = virological response; SVR = sustained virological response.

Predictive factors of SVR in genotype 1b patients

Among 15 patients who completed our protocol with genotype 1b, Potential predictive factors associated with SVR were analyzed. Variables were follow up, the age, gender, body mass index, duration for the initiation of antiviral therapy after transplantation, pretreatment serum HCV RNA levels, immunosuppressive therapy, the number of mutations in the ISDR, HCV core region (double mutant/non-double mutant) adherence of PEGIFN and adherence of RBV.

There was no significance difference between the SVR and non-SVR groups among the 15 patients with genotype 1b in our study (Table III). EVR rates in the SVR group tend to be higher than that of the non-SVR group, albeit that the difference was not significant ($p = 0.07$) (Table III). Mutation of aa 70 and aa 91 in the core region of the HCV protein and fewer mutations in its ISDR region did not significantly differ between the SVR and non-SVR groups among the 15 patients with genotype 1b in our study.

Although it has been reported that mutation of aa 70 and aa 91 in the core region of the HCV protein is predictive of a non-virological response [17,18], all three patients who had double mutation of aa 70 and aa 91 in the core region achieved SVR in this study.

Moreover, although it has also been reported that fewer mutations in the ISDR region of the HCV protein is predictive of a non-virological response [15], all four patients with 0 or 1 mutation in the ISDR achieved SVR.

Discussion

The optimal duration of therapy for liver transplant recipients with recurrent HCV is unclear. The treatment period for immunocompetent patients in the majority of published studies is 48 weeks. Among immunocompetent patients, the probability of relapse was greater in those responding later [23,24]. Using a mathematical model, Drusano and Preston reported that genotype 1-infected patients require the continuous absence of detectable HCV RNA in serum for 36 weeks to attain 90% probabilities of an SVR (i.e. relapse rate 10%) [25]. It is recently recommended that 72-week IFN treatment, compared to 48-week standard IFN treatment, was effective for the untransplanted patients with chronic hepatitis C whose HCV RNA does not reach undetectable level within 12 weeks [11,12]. It is also well known that patients with recurrent chronic hepatitis after LDLT are unlikely to achieve SVR, compared to immunocompetent

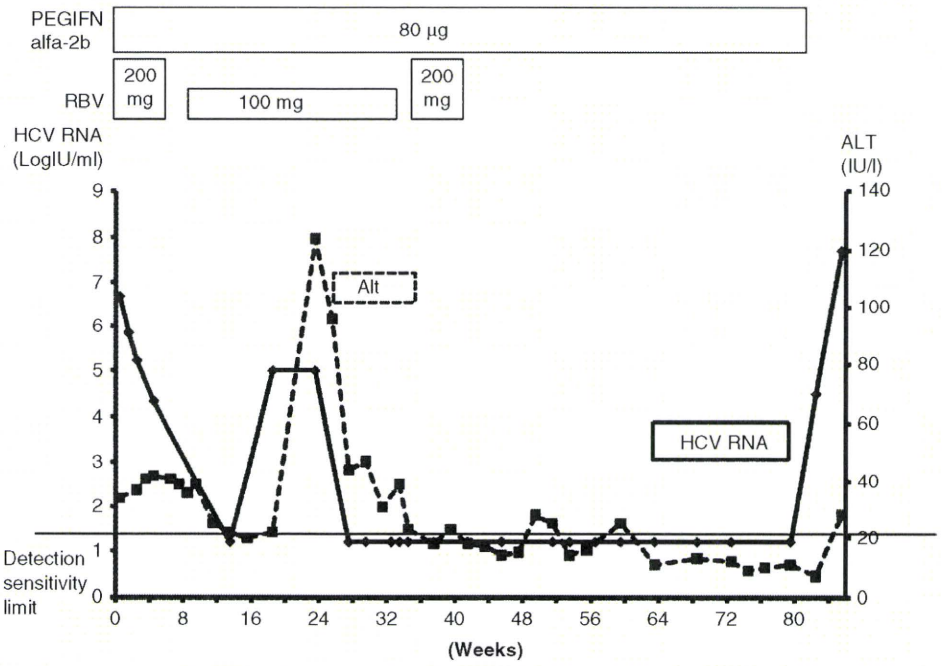

Figure 2. Clinical course in a male patient aged 56 years with genotype 1b, HCV Core 70mutant 91wild, and 0 ISDR mutations. Serum HCV RNA became negative at 27 weeks, after which treatment duration was 52 weeks. However, HCV RNA became positive at 1 week after the cessation of treatment.

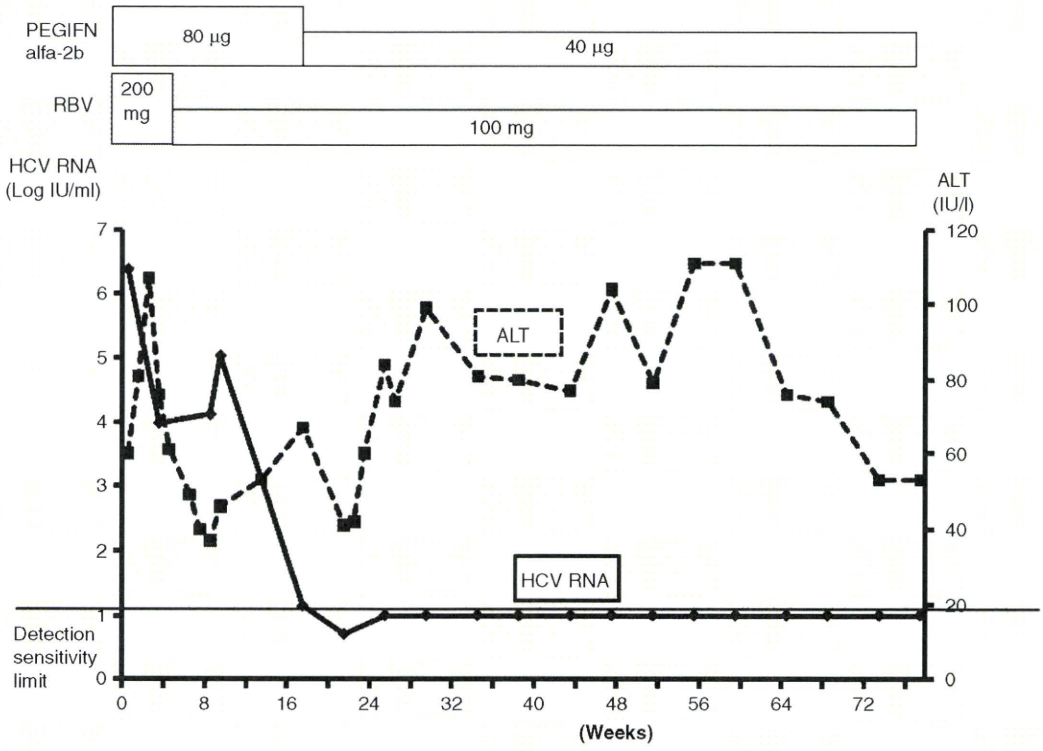

Figure 3. Clinical course in a male patient aged 69 years with genotype 1b, HCV Core 70mutant 91mutant, and 0 ISDR mutations. Virological response occurred at 21 weeks and therapy continued to 78 weeks. Final status was SVR.

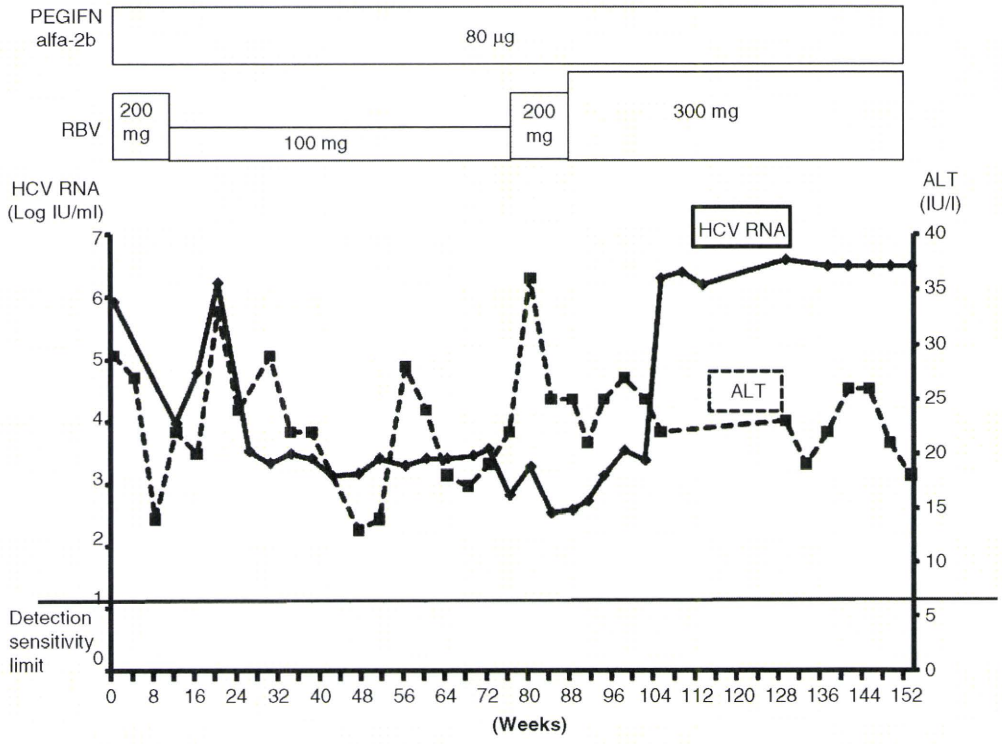

Figure 4. Clinical course in a male patient aged 51 years with genotype 1b, HCV Core 70wild 91wild, and 5 ISDR mutations. He did not develop VR during the dosing period.

untransplanted patients. Consequently, prolonged IFN treatment would be useful and improve the SVR rate for transplanted patients.

We treated recipients with PEGIFN/RBV until HCV RNA had reached undetectable levels and then to continue treatment for at least 1 year. 62.9% of patients (17/27) could complete therapy without severe adverse affects (Figure 1) and relapse rate under this study was 12.5% (Table II), whereas Tamura and Ueda reported a relapse rate of 14% and 3% under the same treatment. As a result, SVR rate was 34% and 50%, respectively [13,14]. With the aid of these results, it might indicate that prolonged PEGIFN/RBV therapy would be useful in eradicating HCV in LDLT patients.

In our study, seven patients achieved SVR by prolonged PEGIFN/RBV for at least 1 year or more. Three of seven patients were EVR and four were LVR.

By contrast, in eight patients who were non-SVR, only one patient had reached undetectable levels of HCV

Table III. Predictive factors associated with SVR in genotype 1b patients.

	SVR (n = 7)	Non-SVR (n = 8)	p-Value
Age (years)*	60 (44–69)	57 (47–65)	0.64
Gender (male/female)	7/0	3/5	0.07
Body mass index*	24.1 (21.4–26.5)	24.2 (18.9–42.2)	0.67
Viral load at therapy (log IU/ml)*	6.3 (5.8–6.6)	6.6 (5.9–7.2)	0.48
Time from transplantation to therapy (months)*	12 (1–41)	3 (3–7)	0.21
Number of mutations in the ISDR (0–1/2–5)	4/3	7/1	0.28
HCV core region (double mutant/non-double mutant)	3/4	3/5	0.6
Duration of treatment (week)*	72 (48–179)	75 (61–133)	0.7
Immunosuppression (tacrolimus/cyclosporine)	6/2	7/1	1
Adherence of PEGIFN (%)*	80 (35.5–100)	71.5 (45.4–100)	0.39
Adherence of RBV (%)*	47.4 (11.2–62.5)	25.5 (15.3–65.9)	0.74
Early virological response (yes/no)	3/4	0/8	0.07

*Values are median (range).

RNA and other seven patients had never reached undetectable levels of HCV RNA. That is, if patients had reached undetectable levels of HCV RNA, they could eradicate HCV RNA in the liver tissue by prolonged IFN therapy for more than 48 weeks after HCV RNA reached undetectable levels. This regimen is similar to that of a recent recommendation that PEGIFN/RBV therapy for 72 weeks is necessary for patients with chronic hepatitis C whose HCV RNA does not reach undetectable levels within 12 weeks.

Recent findings among immunocompetent patients of pretreatment factors that could predict treatment efficacy of 72-week PEGIFN/RBV identified substitution of either or both aa 70 or 91 in the HCV core region, and the number of substitutions in amino acids 2209–2248, the ISDR of NS5A in HCV genotype 1b [26]. By contrast, however, our present results showed that substitution of aa 70 and/or 91 in the HCV core region or the number of ISDR were not predictive of SVR (Table III). All three patients who had double mutation of aa 70 and aa 91 in core region of HCV protein achieved SVR in this study, as did all four patients whose number of mutations in the ISDR was 0 or 1 (Table II).

Recently Fukuhara et al. reported that mutations of the HCV core and NS5A regions of HCV genome were associated with the SVR rates in 50 patients [27]. Although the number of our patients included was less than Fukuhara's, we think that our result is still worth reporting because, in the case of acute hepatitis C, 24-week IFN treatment is enough to eradicate HCV in most cases, suggesting that HCV core mutant and the substitutions of amino acids of the HCV NS5A region are not likely to affect the SVR rate for acute hepatitis C. Since the recurrence of hepatitis C for transplanted patients is another acute hepatitis C, those substitutions might not affect the SVR rate of IFN treatment. Further studies would reveal whether the mutations of the HCV core and NS5A regions of HCV genome were associated with the SVR rates.

Only one patient had HCV relapse after 79 weeks treatment, a male aged 56 years with genotype 1b, HCV Core 70mutant 91wild and number of ISDR mutation 0 (Figure 2). He had a VR at 27 weeks, which lasted for 52 weeks, and continued therapy to 79 weeks. However, he subsequently experienced relapse of HCV. One of many possible reasons was likely low adherence to RBV (7%).

Several reasons may account for the lack of association of HCV core region mutation and number of ISDR mutations with SVR rate. One reason is that it is acute hepatitis after LDLT, which is usually treated as soon as possible: even in those infected with genotype 1, HCV could be eradicated with regular IFN for 24 weeks after acute infection [28–31], meaning that mutation of the core region and NS5A could not be determinants of PEGIFN therapy in LDLT cases. A second reason might be poor adherence to PEGIFN and RBV treatment in patients with LDLT. Among patients who experience severe leucocytopenia, thrombocytopenia and anemia after LDLT, dose reductions in PEGIFN or RBV are therefore inevitable. Therefore, it is reasonable to prolong the duration of PEGIFN/RBV therapy. Taken together, recurrent hepatitis C after LDLT is different from hepatitis C in immunocompetent patients. This might be the reason why any predictive factor but EVR was an only predictive factor of SVR in this study.

There were several limitations in present study. One was that our study is retrospective.

Since it was scheduled that the end point of treatment should be 1 year after serum HCV RNA became negative, it compelled to design the retrospective study as a pilot study. Further prospective study will prove our protocol strongly and help achieving high SVR and low relapse rate. Another limitation was the low number of patients included. Although other institutes also demonstrated good results with similar interferon protocol, as mentioned above [13,14], another study with more number of patients will prove the consistence of our study.

In conclusion, for recurrent hepatitis C after LDLT, our findings indicate that PEGIFN therapy for at least 1 year after HCV RNA reaches undetectable levels might prevent HCV viral relapse. Combination of the new selective inhibitors of HCV, named STAT-C (specifically targeted antiviral therapy for HCV), is expected to further improvements in SVR rates.

Acknowledgements

The authors thank Rie Akiyama and Hiromi Abe for their excellent technical assistance.

Declaration of interest: The authors report no conflicts of interest. The authors alone are responsible for the content and writing of the paper.

References

[1] Samuel D, Muller R, Alexander G, Fassati L, Ducot B, Benhamou JP, et al. Liver transplantation in European patients with the hepatitis B surface antigen. N Engl J Med 1993;329:1842–7.

[2] Forman LM, Lewis JD, Berlin JA, Feldman HI, Lucey MR. The association between hepatitis C infection and survival after orthotopic liver transplantation. Gastroenterology 2002; 122:889–96.

[3] Ueda Y, Takada Y, Haga H, Nabeshima M, Marusawa H, Ito T, et al. Limited benefit of biochemical response to combination therapy for patients with recurrent hepatitis C

after living-donor liver transplantation. Transplantation 2008;85:855–62.

[4] Sugawara Y, Makuuchi M, Matsui Y, Kishi Y, Akamatsu N, Kaneko J, et al. Preemptive therapy for hepatitis C virus after living-donor liver transplantation. Transplantation 2004;78: 1308–11.

[5] Sugawara Y, Makuuchi M. Living donor liver transplantation to patients with hepatitis C virus cirrhosis. World J Gastroenterol 2006;12:4461–5.

[6] Roche B, Sebagh M, Canfora ML, Antonini T, Roque-Afonso AM, Delvart V, et al. Hepatitis C virus therapy in liver transplant recipients: response predictors, effect on fibrosis progression, and importance of the initial stage of fibrosis. Liver Transpl 2008;14:1766–77.

[7] Lodato F, Berardi S, Gramenzi A, Mazzella G, Lenzi M, Morelli MC, et al. Clinical trial: peg-interferon alfa-2b and ribavirin for the treatment of genotype-1 hepatitis C recurrence after liver transplantation. Aliment Pharmacol Ther 2008;28:450–7.

[8] Dinges S, Morard I, Heim M, Dufour JF, Mullhaupt B, Giostra E, et al. Pegylated interferon-alpha2a/ribavirin treatment of recurrent hepatitis C after liver transplantation. Transpl Infect Dis 2009;11:33–9.

[9] Saab S, Oh MK, Ibrahim AB, Durazo F, Han S, Yersiz H, et al. Anemia in liver transplant recipients undergoing antiviral treatment for recurrent hepatitis C. Liver Transpl 2007;13:1032–8.

[10] Sugawara Y, Makuuchi M. Living donor liver transplantation for patients with hepatitis C virus cirrhosis: Tokyo experience. Clin Gastroenterol Hepatol 2005;3(10 Suppl 2):S122–4.

[11] Berg T, von Wagner M, Nasser S, Sarrazin C, Heintges T, Gerlach T, et al. Extended treatment duration for hepatitis C virus type 1: comparing 48 versus 72 weeks of peginterferon-alfa-2a plus ribavirin. Gastroenterology 2006;130:1086–97.

[12] Pearlman BL, Ehleben C, Saifee S. Treatment extension to 72 weeks of peginterferon and ribavirin in hepatitis c genotype 1-infected slow responders. Hepatology 2007;46: 1688–94.

[13] Tamura S, Sugawara Y, Yamashiki N, Kaneko J, Kokudo N, Makuuchi M. Pre-emptive antiviral therapy in living donor liver transplantation for hepatitis C: observation based on a single-center experience. Transpl Int 2009;23:580–8.

[14] Ueda Y, Takada Y, Marusawa H, Egawa H, Uemoto S, Chiba T. Individualized extension of pegylated interferon plus ribavirin therapy for recurrent hepatitis C genotype 1b after living-donor liver transplantation. Transplantation 2010 (In press).

[15] Enomoto N, Sakuma I, Asahina Y, Kurosaki M, Murakami T, Yamamoto C, et al. Mutations in the nonstructural protein 5A gene and response to interferon in patients with chronic hepatitis C virus 1b infection. N Engl J Med 1996;334:77–81.

[16] Akuta N, Suzuki F, Sezaki H, Suzuki Y, Hosaka T, Someya T, et al. Predictive factors of virological non-response to interferon-ribavirin combination therapy for patients infected with hepatitis C virus of genotype 1b and high viral load. J Med Virol 2006;78:83–90.

[17] Akuta N, Suzuki F, Kawamura Y, Yatsuji H, Sezaki H, Suzuki Y, et al. Predictive factors of early and sustained responses to peginterferon plus ribavirin combination therapy in Japanese patients infected with hepatitis C virus genotype 1b: amino acid substitutions in the core region and low-density lipoprotein cholesterol levels. J Hepatol 2007;46:403–10.

[18] Akuta N, Suzuki F, Sezaki H, Suzuki Y, Hosaka T, Someya T, et al. Association of amino acid substitution pattern in core protein of hepatitis C virus genotype 1b high viral load and non-virological response to interferon-ribavirin combination therapy. Intervirology 2005;48:372–80.

[19] Berenguer M, Palau A, Fernandez A, Benlloch S, Aguilera V, Prieto M, et al. Efficacy, predictors of response, and potential risks associated with antiviral therapy in liver transplant recipients with recurrent hepatitis C. Liver Transpl 2006;12:1067–76.

[20] Hanouneh IA, Miller C, Aucejo F, Lopez R, Quinn MK, Zein NN. Recurrent hepatitis C after liver transplantation: on-treatment prediction of response to peginterferon/ribavirin therapy. Liver Transpl 2008;14:53–8.

[21] Akuta N, Suzuki F, Kawamura Y, Yatsuji H, Sezaki H, Suzuki Y, et al. Predictors of viral kinetics to peginterferon plus ribavirin combination therapy in Japanese patients infected with hepatitis C virus genotype 1b. J Med Virol 2007;79:1686–95.

[22] Kato N, Hijikata M, Ootsuyama Y, Nakagawa M, Ohkoshi S, Sugimura T, et al. Molecular cloning of the human hepatitis C virus genome from Japanese patients with non-A, non-B hepatitis. Proc Natl Acad Sci USA 1990;87:9524–8.

[23] Ferenci P, Fried MW, Shiffman ML, Smith CI, Marinos G, Goncales FL Jr, et al. Predicting sustained virological responses in chronic hepatitis C patients treated with peginterferon alfa-2a (40 KD)/ribavirin. J Hepatol 2005;43: 425–33.

[24] Zeuzem S, Buti M, Ferenci P, Sperl J, Horsmans Y, Cianciara J, et al. Efficacy of 24 weeks treatment with peginterferon alfa-2b plus ribavirin in patients with chronic hepatitis C infected with genotype 1 and low pretreatment viremia. J Hepatol 2006;44:97–103.

[25] Drusano GL, Preston SL. A 48-week duration of therapy with pegylated interferon alpha 2b plus ribavirin may be too short to maximize long-term response among patients infected with genotype-1 hepatitis C virus. J Infect Dis 2004;189:964–70.

[26] Akuta N, Suzuki F, Hirakawa M, Kawamura Y, Yatsuji H, Sezaki H, et al. A matched case-controlled study of 48 and 72 weeks of peginterferon plus ribavirin combination therapy in patients infected with HCV genotype 1b in Japan: amino acid substitutions in HCV core region as predictor of sustained virological response. J Med Virol 2009;81:452–8.

[27] Fukuhara T, Taketomi A, Okano S, Ikegami T, Soejima Y, Shirabe K, et al. Mutations in hepatitis C virus genotype 1b and the sensitivity of interferon-ribavirin therapy after liver transplantation. J Hepatol 2010;52:672–80.

[28] Kamal SM, Fouly AE, Kamel RR, Hockenjos B, Al Tawil A, Khalifa KE, et al. Peginterferon alfa-2b therapy in acute hepatitis C: impact of onset of therapy on sustained virologic response. Gastroenterology 2006;130:632–8.

[29] Ogata K, Ide T, Kumashiro R, Kumada H, Yotsuyanagi H, Okita K, et al. Timing of interferon therapy and sources of infection in patients with acute hepatitis C. Hepatol Res 2006;34:35–40.

[30] Delwaide J, Bourgeois N, Gerard C, De Maeght S, Mokaddem F, Wain E, et al. Treatment of acute hepatitis C with interferon alpha-2b: early initiation of treatment is the most effective predictive factor of sustained viral response. Aliment Pharmacol Ther 2004;20:15–22.

[31] Jaeckel E, Cornberg M, Wedemeyer H, Santantonio T, Mayer J, Zankel M, et al. Treatment of acute hepatitis C with interferon alfa-2b. N Engl J Med 2001;345:1452–7.

Immunological Property of Antibodies against *N*-Glycolylneuraminic Acid Epitopes in Cytidine Monophospho–*N*-Acetylneuraminic Acid Hydroxylase-Deficient Mice

Hiroyuki Tahara,* Kentaro Ide,* Nabin Bahadur Basnet,* Yuka Tanaka,* Haruo Matsuda,† Hiromu Takematsu,‡ Yasunori Kozutsumi,‡ and Hideki Ohdan*

The generation of pigs devoid of Galα1,3Galβ1,4GlcNAc (Gal) residues has stimulated interest in non-Gal Ags as potentially important targets for Ab binding leading to rejection of pig organ xenografts in humans. Although *N*-glycolylneuraminic acid (NeuGc) epitopes, which are widely expressed on the endothelial cells of all mammals except humans, are likely targets of anti–non-Gal Abs, this aspect has not been investigated intensively owing to the absence of an appropriate animal model. In this study, we used $CMAH^{-/-}$ mice, which are completely deficient in NeuGc and thus produce anti-NeuGc Abs. Sera obtained from $CMAH^{-/-}$ mice and healthy human volunteers having anti-NeuGc Abs initiated complement-mediated lysis against $CMAH^{+/+}$ cells in vitro. The cytotoxic activity of anti-NeuGc Abs was also determined in vivo (i.e., NeuGc-expressing $CMAH^{+/+}$ mouse splenocytes that had been i.v. injected were completely eliminated in syngeneic $CMAH^{-/-}$ mice). $CMAH^{-/-}$ mice rejected the islets transplanted from syngeneic $CMAH^{+/+}$ mice. Thus, the anti-NeuGc Ab-mediated response may be crucially involved in xenograft loss. This is the first direct demonstration of the immunogenic property of NeuGc determinants as targets of the corresponding Abs in $CMAH^{+/+}$-to-$CMAH^{-/-}$ transplantation setting. *The Journal of Immunology*, **2010, 184: 3269–3275.**

Xenotransplantation of pig organs into humans is a potential solution to the shortage of donor organs for transplantation (1). Humans lack a functional *GalT* gene; thus, they do not express Galα1,3Galβ1,4GlcNAc (Gal) carbohydrate residues and produce abundant natural Abs to the Gal epitope (2, 3). These anti-Gal Abs are a major barrier to the xenotransplantation of pig organs into humans because hyperacute rejection (HAR), which occurs in a few minutes or hours, is initiated by the binding of these Abs to Gal determinants that are ubiquitously present on porcine cells (4, 5). Recently, pigs knocked out for the gene encoding *GalT* ($GalT^{-/-}$ pigs), which is responsible for the generation of the Gal epitope, have been cloned (6, 7). The availability of $GalT^{-/-}$ pigs has facilitated longer survival of nonhuman primate recipients with less immune modulation (8, 9). Thus, the absence of Gal expression has led to a substantial advance in addressing HAR; however, another study has shown that acute vascular rejection is caused by induced Abs to Ags other than the Gal epitope (non-Gal Ags) in a $GalT^{-/-}$ pig-to-baboon kidney transplantation model (10). Therefore, the identification and characterization of non-Gal Ags have become a major focus of interest following the generation of $GalT^{-/-}$ pigs (11, 12).

In addition to the non-Gal Ags that might be defined in the $GalT^{-/-}$ pig-to-nonhuman primate model, *N*-glycolylneuraminic acid (NeuGc) epitopes, the so-called Hanganutziu-Deicher Ag (13–15), might act as an additional barrier, resulting in either HAR or acute vascular rejection of xenografts even from $GalT^{-/-}$ pigs, to the eventual clinical application in humans. The most common mammalian sialic acids, which are components of the carbohydrate chains of glycoconjugates and are involved in cell–cell recognition and cell–pathogen interactions, are a group of carbohydrates of two main forms: *N*-acetylneuraminic acid and NeuGc. NeuGc is generated by the hydroxylation of CMP-Neu5Ac to CMP-Neu5Gc catalyzed by the enzyme cytidine monophospho–*N*-acetylneuraminic acid hydroxylase (*CMAH*). NeuGc epitopes are widely expressed on the endothelial cells of all mammals except humans (16) and are considered to be potential porcine targets for preformed and elicited anti–non-Gal Abs in humans (17–19), but not in baboons, that express these epitopes (16, 20). Anti-NeuGc Abs to porcine RBCs are detectable in the sera of 85% of healthy humans (17). There is a significant correlation between anti–non-Gal and anti-NeuGc Abs of both human IgM and IgG classes, and anti-NeuGc Abs constitute a significant portion of anti–non-Gal Abs (21). The presence of anti-NeuGc Abs in most normal human sera may well constitute an immunological hurdle, thereby contributing to Ab-mediated rejection; this is because the NeuGc epitope is expressed on most porcine cells, including vascular endothelial cells (22). However, this aspect has not been investigated

*Division of Frontier Medical Science, Programs for Biomedical Research, Department of Surgery, Graduate School of Biomedical Science and †Laboratory of Immunobiology, Department of Molecular and Applied Bioscience, Graduate School of Biosphere Science, Hiroshima University, Hiroshima; and ‡Laboratory of Membrane Biochemistry and Biophysics, Graduate School of Biostudies, Kyoto University, Kyoto, Japan

Received for publication August 28, 2009. Accepted for publication December 31, 2009.

This work was supported by a Grand-in-Aid for Sciences Research (B) from the Japan Society for the Promotion of Science, a Grand-in-Aid for Young Scientists (Start-up) from the Japan Society for the Promotion of Science, and the Takeda Science Foundation. This work was carried out at the Analysis Center of Life Science (Hiroshima University).

Address correspondence and reprint requests to Dr. Hideki Ohdan, Division of Frontier Medical Science, Programs for Biomedical Research, Department of Surgery, Graduate School of Biomedical Science, Hiroshima University 1-2-3 Kasumi, Minami-Ku, Hiroshima 734-8551, Japan. E-mail address: hohdan@hiroshima-u.ac.jp

The online version of this article contains supplemental material.

Abbreviations used in this paper: B6, C57BL/6J; CMAH, cytidine monophospho–*N*-acetylneuraminic acid hydroxylase; FCM, flow cytometry; Gal, Galα1,3-Galβ1,4GlcNAc; GalT, α1,3-galactosyltransferase; HAR, hyper acute rejection; iEQ, islet equivalent; NAbs, natural Abs; NeuGc, *N*-glycolylneuraminic acid; WT, wild-type.

www.jimmunol.org/cgi/doi/10.4049/jimmunol.0902857

intensively owing to the absence of an appropriate animal model. Recently, we generated mice homozygous for a null *CMAH* allele by targeted disruption of the murine *CMAH* gene (23). In this study, we present in vitro and in vivo evidence for the cytotoxicity of non-Gal Abs against NeuGc epitopes using $CMAH^{-/-}$ mice, which are completely deficient in NeuGc.

Materials and Methods

Animals, cells, and immunization

C57BL/6J (B6) (H-2^b) (syngeneic $CMAH^{+/+}$) mice, BALB/c (H-2^d) mice, and F344 rats were purchased from CLEA Japan (Tokyo, Japan) and housed in the animal facility of Hiroshima University in a specific pathogen-free microisolator environment. These mice and rats were used at an age of 8 to 16 wk. $CMAH^{-/-}$ mice (23) in a B6 background (backcrossed to B6 for >10 generations), which are completely deficient in NeuGc, and $GalT^{-/-}$ mice (24) in a B6 background (backcrossed seven times to B6), in which Gal expression is completely eliminated and in which naturally occurring anti-Gal Abs are present in the sera, were kindly provided by Dr. M. Sykes, Massachusetts General Hospital, Boston, MA. The porcine endothelial cell line MYP30 (25) was kindly provided by Dr. S. Miyagawa, Osaka University, Osaka, Japan. To elicit anti-NeuGc Ab production, $CMAH^{-/-}$ mice were i.p. immunized twice with NeuGc-expressing cells (i.e., thymocytes) obtained from syngeneic $CMAH^{+/+}$ B6 mice, allogeneic BALB/c mice, or xenogeneic F344 rats, or with xenogeneic porcine MYP30 cells, at an interval of 1 wk (10^7 cells/mouse at each immunization). The thymocytes or MYP30 cells were washed twice and resuspended at 10^7/ml in medium 199 (Sigma-Aldrich, St. Louis, MO) containing 1% HEPES buffer (Life Technologies, Carlsbad, CA) and 0.08 μg/ml gentamycin (Sigma-Aldrich) before injection. All experiments were approved by the Institutional Review Board of Hiroshima University and conducted in accordance with the guidelines of the National Institutes of Health.

Immunohistochemistry

Multiple tissues from wild-type (WT) $CMAH^{+/+}$ B6 mice, $GalT^{-/-}$ mice, and $CMAH^{-/-}$ mice were analyzed for the expression of NeuGc epitopes by immunohistochemistry using a standard immunoperoxidase technique. The tissues were fixed with formaldehyde. Prior to staining, endogenous peroxidase activity was quenched, and nonspecific binding sites were blocked with normal goat serum in PBS for 30 min. Sections were then incubated with a chicken monoclonal anti-NeuGc Ab at 4°C overnight (chickens are CMAH-deficient). After washing the sections, biotin-conjugated goat anti-chicken IgY (H&L) polyclonal Ab (Abcam, Cambridge, MA) in PBS at a 1:100 dilution was applied for 30 min. Sections of islet grafts from $CMAH^{+/+}$ or $CMAH^{-/-}$ mice were incubated with guinea pig polyclonal Ab to insulin (Abcam). Biotin-conjugated goat polyclonal Ab to guinea pig IgG (Abcam) was used to detect insulin. After washing the sections, HRP-conjugated streptavidin (Histofine SAB-PO Kit; Nichirei, Tokyo, Japan) was applied for 30 min. Peroxidase activity was visualized by staining with 3,3′-diaminobenzidine (Muto Pure Chemicals, Tokyo, Japan) for 10 min in combination with H&E counterstaining.

Pools of isolated islets from $CMAH^{+/+}$ or $CMAH^{-/-}$ mice were fixed with cold acetone and frozen for immunofluorescence staining. The cryosections were incubated with $CMAH^{-/-}$ mouse sera containing anti-NeuGc Abs, and then FITC-conjugated goat anti-mouse IgM (Vector Laboratories, Burlingame, CA) and IgG (Zymed, Invitrogen, Carlsbad, CA) were applied.

Flow cytometry analysis for detecting NeuGc Ags and anti-NeuGc Abs

All flow cytometry (FCM) analyses were performed using a FACSCalibur dual-laser flow cytometer (BD Biosciences, San Jose, CA). The expression of NeuGc epitopes on the surface of hematopoietic cells (RBCs, bone marrow cells, splenocytes, and thymocytes) in WT, $GalT^{-/-}$, and $CMAH^{-/-}$ mice was analyzed. These cells were incubated with a chicken mAb specific for NeuGc epitopes. The cells were then washed, incubated with FITC-conjugated goat anti-chicken IgG (Bethyl Laboratories, Montgomery, TX), and subjected to FCM analysis. Indirect immunofluorescence staining of thymocytes from syngeneic $CMAH^{+/+}$ B6 mice was used to detect anti-NeuGc Abs. To elicit the production of anti-NeuGc Abs, $CMAH^{-/-}$ mice were sensitized with NeuGc-expressing thymocytes obtained from $CMAH^{+/+}$ syngeneic B6 mice, allogenic BALB/c mice, xenogeneic F344 rats, or porcine MYP30 cells. NeuGc-expressing thymocytes (1.0×10^6 cells) were incubated with 10 μl mouse serum, washed, incubated with PE-conjugated rat anti-mouse IgM, IgG1, IgG2a/2b, and IgG3 monoclonal Abs (BD Biosciences), and subjected to FCM analysis.

In vitro Ab-dependent cytotoxicity assay

Serum samples from $CMAH^{-/-}$ mice and healthy human volunteers were incubated for 30 min at 56°C to inactivate complement. The samples were serially diluted with RPMI 1640 medium (plus 10% FBS; Biological Industries, Beit Haemek, Israel). Thymocytes of $CMAH^{+/+}$ or $CMAH^{-/-}$ B6 mice used as target cells were labeled with [^{51}Cr] (4 μCi/well) for 60 min at 37°C. Labeled cells were washed three times and loaded onto round-bottomed 96-well microtiter plates (BD Biosciences) at a density of 1.0×10^6 cells (80 μl per well) (suspended in RPMI 1640 medium plus 10% FBS). The labeled cells were incubated with 80 μl diluted $CMAH^{-/-}$ mice serum for 30 min at 4°C. Postincubation, the cells were washed and further incubated with 40 μl of 20% rabbit complement (Cedarlane Laboratories, Burlington, Ontario, Canada) for 45 min at 37°C. Negative controls used as target cells were incubated with medium and complement alone in the absence of serum, whereas positive controls cells lysed with 2% Nonidet P-40 (Nacalai Tesque, Kyoto, Japan) to determine the maximum [^{51}Cr] release. Postincubation, the plates were centrifuged, and the cell-free supernatants were carefully harvested. The release of radioactive [^{51}Cr] was analyzed using a γ counter (ARC-370M; Aloka, Wallingford, CT), and the percentage of specific lysis was calculated as follows: % specific lysis = ([A − B])/([C − B]) × 100, where A represents the experimental release (cpm in the supernatant from target cells incubated with serum and complement), B is the spontaneous release (cpm in the supernatant from target cells incubated with medium and complement alone), and C is the maximum release (cpm released from target cells as positive controls). The spontaneous release was <10% of the maximum release. Each experiment was performed in triplicate.

In vivo cytotoxicity assay

Splenocytes were prepared from WT $CMAH^{+/+}$ B6 mice and resuspended in PBS. CFSE (Molecular Probes, Eugene, OR) was added to give a final concentration of 5 μM, and the cells were gently mixed and incubated for 5 min at 37°C in a CO_2 incubator protected from light. Labeling of cells was terminated by adding cold PBS containing 2% FBS, and the cells were then washed and resuspended in medium 199 containing 1% HEPES buffer and 0.08 μg/ml gentamycin. NeuGc-expressing splenocytes labeled with CFSE (2.0×10^7 cells in 0.5 ml) were injected i.v. into $CMAH^{+/+}$ or $CMAH^{-/-}$ B6 mice in which anti-NeuGc Abs had been induced by immunization with rat thymocytes. The prospective recipient mice were irradiated with 6 Gy/whole body to facilitate the efficient engraftment of target cells. Splenocytes were collected from each recipient mouse 7 d postinoculation, and single-cell suspensions were prepared and analyzed by FCM. The percentage of surviving CFSE-labeled splenocytes from each recipient mouse was calculated.

Islet transplantation

$CMAH^{+/+}$ or $CMAH^{-/-}$ B6 mice immunized with rat thymocytes were rendered diabetic through a single i.p. administration of 170 mg/kg streptozotocin (Sigma-Aldrich) at 6 d before islet transplantation. The diabetic mice that had nonfasting blood glucose levels of >400 mg/dl on the day of transplantation were used as the recipients. The blood glucose levels were monitored intermittently with a blood glucose test meter (Medisafe-mini GR-102; Terumo, Somerset, NJ). When no islet transplantation was performed, the diabetes persisted in all the diabetic mice (blood glucose level, >350 mg/dl), and no spontaneous reversal of diabetes was observed for at least the next 3 mo. The donors were WT $CMAH^{+/+}$ B6 females aged 10–12 wk. The pancreas was isolated after common bile duct perfusion of 4°C collagenase P (1 mg/ml; Roche, Somerville, NJ) in HBSS (Life Technologies), which was followed by incubation of the distended pancreas in a 37°C water bath for 20 min to achieve mechanical disruption. The pancreatic islets were purified on a Percoll (GE Healthcare, Piscataway, NJ) density gradient. Postisolation, 200, 350, or 500 $CMAH^{+/+}$ islet equivalents (iEQs; diameter >150 μm) were handpicked and immediately transplanted into the recipient left renal subcapsular space.

Heterotopic heart transplantation

Neonatal F344 rat (10–14 d old) heart xenografts or $CMAH^{+/+}$ syngeneic B6 mouse (14–16 wk old) heart grafts were transplanted. Cervical heterotopic heart transplantation was performed using the cuff technique modified from a previously described method (26). Briefly, the right external jugular vein and right common carotid artery of recipients were dissected free, mobilized as far as possible, and fixed to the appropriate cuffs. The cuffs were composed of polyethylene tubes (2.5 Fr; Portex, Smiths Medical, Watford, U. K.), the diameters of which were adjusted by physical extension. For anastomoses, the aorta and the main pulmonary artery of the harvested donor hearts were drawn over the end of the common carotid artery and the external jugular vein, respectively. To enhance anti-NeuGc Ab production,

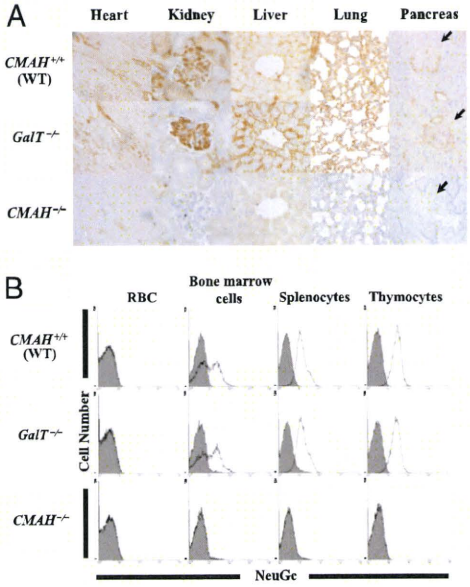

FIGURE 1. The detection of NeuGc expression in multiple tissues and on the surface of hematopoietic cells. *A*, NeuGc expression was studied by immunohistochemistry in multiple tissues (heart, kidney, liver, lung, and pancreas [islets are indicated by arrows]) from WT $CMAH^{+/+}$, $GalT^{-/-}$, and $CMAH^{-/-}$ mice using a chicken anti-NeuGc mAb, and examples are shown. $CMAH^{-/-}$ mice are completely deficient in NeuGc. Original magnification ×200. *B*, The expression of NeuGc epitopes on the surface of hematopoietic cells (RBCs, bone marrow cells, splenocytes, and thymocytes) was analyzed using FCM. These cells were incubated with a sensitive chicken polyclonal Ab specific for NeuGc epitopes followed by incubation with anti-chicken IgG. Expression of NeuGc was also completely absent in $CMAH^{-/-}$ mice. The filled histogram represents a negative control stained with secondary Ab alone.

$CMAH^{-/-}$ recipients were immunized by injection with 10^7 porcine MYP30 cells at 8 wk before heart transplantation. To increase lymphocytotoxic activity against recipient peripheral lymphocytes in the presence of anti-NeuGc Abs, 0.5 ml rabbit complement (Cedarlane Laboratories) was injected to the recipient jugular vein just before anastomosis of the graft. The graft ischemic time for the transplanted hearts was <30 min. The function of the grafts was monitored by daily inspection and palpation. Rejection was determined by the cessation of beating of the graft and was confirmed by histology.

Statistical analysis

The results were statistically analyzed using unpaired or paired Student *t* tests of means or the log-rank test where appropriate. A p value of < 0.05 was considered to be statistically significant.

Results

NeuGc epitopes were expressed on vascular endothelial cells, thymocytes, and splenocytes in wild-type $CMAH^{+/+}$ *and* $GalT^{-/-}$ *mice but were not detected in* $CMAH^{-/-}$ *mice*

In pigs, NeuGc epitopes are ubiquitously expressed on the vascular endothelial cells of the kidney, heart, liver, pancreas, lung, etc. (16). NeuGc epitopes are expressed on porcine aortic endothelial cells at a similar level to Gal epitopes, the number of which was previously reported as 2.0×10^7/cell (27). It has been reported that the extent of glycoconjugate sialylation with NeuGc is very variable and dependent on the species, tissue, and developmental stage (28). Although NeuGc was easily detectable on the vascular endothelial cells of all analyzed tissues in WT $CMAH^{+/+}$ mice (i.e., lung, heart, liver, kidney, and pancreas), we were unable to detect this epitope in any tissues of the $CMAH^{-/-}$ mice (Fig. 1*A*). The expression of NeuGc was analyzed on the surface of hematopoietic cells by FCM. The

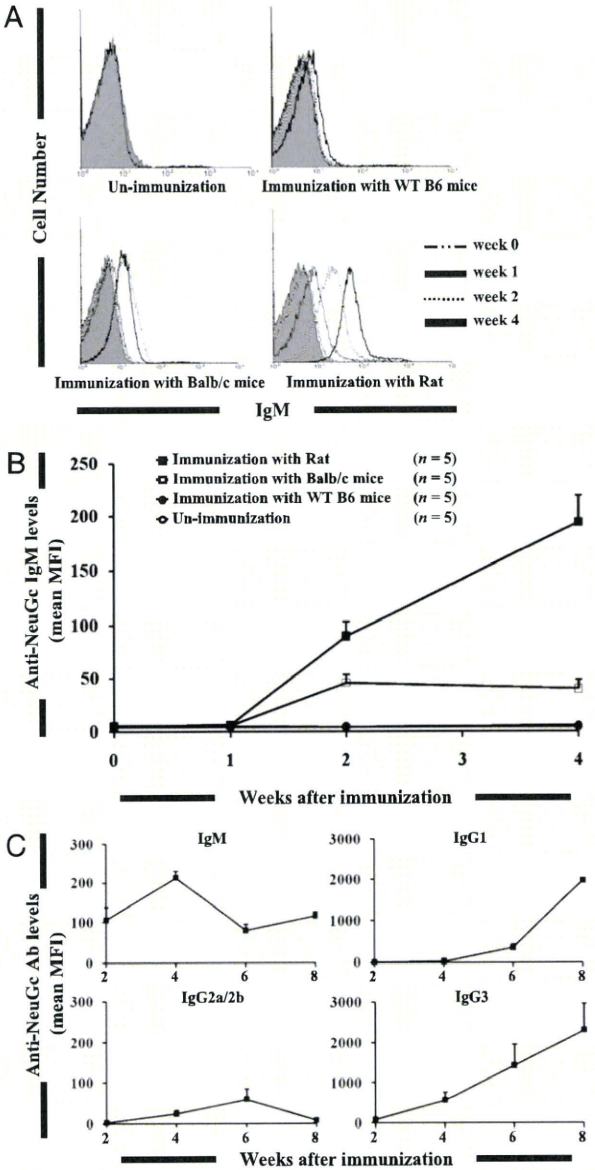

FIGURE 2. The detection of anti-NeuGc Abs. *A*, Anti-NeuGc NAbs were not detected in $CMAH^{-/-}$ mice. The FCM profiles shown are from representative experiments examining anti-NeuGc IgM titers at 0, 1, 2, and 4 wk postimmunization with thymocytes. The filled histogram represents a negative control stained with PE-conjugated rat anti-mouse mAb alone. *B*, The kinetics of the means of anti-NeuGc IgM titers (n = 5 in each group) is shown for $CMAH^{-/-}$ mice at 0, 1, 2, and 4 wk after their sensitization with syngeneic, allogeneic, or xenogeneic NeuGc-expressing thymocytes. The mean ± SEM of five experiments are shown. *C*, $CMAH^{-/-}$ mice can produce anti-NeuGc IgM and IgG after their sensitization with xenogeneic NeuGc-expressing rat thymocytes. A few months later, various isotypes of anti-NeuGc Ab in the sera were quantified by FCM (n = 5). The mean ± SEM of five independent experiments is shown.

RBCs of WT $CMAH^{+/+}$ mice did not express NeuGc. However, their splenocytes and thymocytes did exhibit remarkable NeuGc expression. In contrast, we were unable to detect any NeuGc expression on these cells in $CMAH^{-/-}$ mice (Fig. 1*B*). NeuGc expression was also confirmed on various tissues and cells in $GalT^{-/-}$ mice at a level similar to that in $CMAH^{+/+}$ mice [consistent with observations in $GalT^{-/-}$ pigs (29)], which rules out the possibility that the genetic disruption of *GalT* interferes with NeuGc expression.

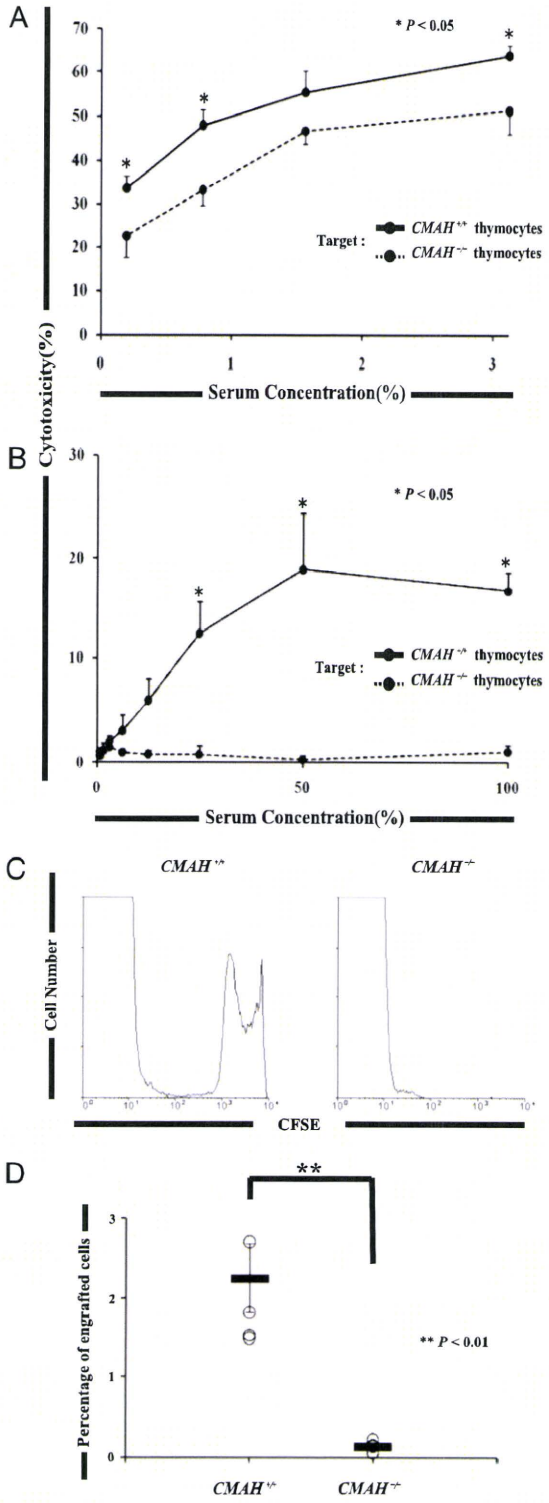

FIGURE 3. In vitro and in vivo Ab-mediated cytotoxicity assays. The results of an in vitro Ab-dependent cytotoxicity assay of sera obtained from healthy human volunteers ($n = 7$) (*A*) or $CMAH^{-/-}$ mice having anti-NeuGc Abs (*B*) against thymocytes obtained from $CMAH^{+/+}$ or $CMAH^{-/-}$ B6 mice are shown. Significantly higher lysis of NeuGc-expressing thymocytes was observed when compared with that of thymocytes lacking NeuGc. The mean ± SEM of five independent experiments is shown. $*p < 0.05$. *C*, In vivo cytotoxicity assay in $CMAH^{+/+}$ or $CMAH^{-/-}$ B6 mice, which were immunized with NeuGc-expressing rat thymocytes, against CFSE-labeled splenocytes from $CMAH^{+/+}$ syngeneic B6 mice. Representative FCM results are shown. *D*, The percentage of engrafted cells labeled with CFSE in the recipient splenocytes ($n = 5$, respectively). Each open circle represents an individual mouse. The mean ± SEM of five experiments is shown. $**p < 0.01$.

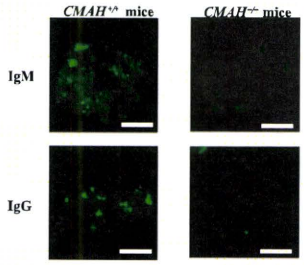

FIGURE 4. Deposition of anti-NeuGc IgM and IgG Ab in the islets isolated from $CMAH^{+/+}$ or $CMAH^{-/-}$ mice. Pictures shown are representative of the single islet from each mouse. Original magnification ×200. Scale bars, 50 μm.

CMAH$^{-/-}$ *mice produced anti-NeuGc Abs postimmunization with NeuGc-expressing cells*

Naturally occurring Abs against NeuGc epitopes were undetectable in the sera of $CMAH^{-/-}$ mice. Furthermore, the elicited anti-NeuGc IgM was barely detectable several weeks postimmunization with NeuGc-expressing thymocytes obtained from $CMAH^{+/+}$ syngeneic B6 mice. The production of anti-NeuGc IgM was significantly more pronounced when $CMAH^{-/-}$ mice were immunized with thymocytes obtained from either $CMAH^{+/+}$ allogenic BALB/c mice or xenogeneic F344 rats (Fig. 2*A*, 2*B*). The production of anti-NeuGc IgG was observed a few months postimmunization with xenogeneic rat thymocytes (predominant subclasses were IgG1 and IgG3) (Fig. 2*C*), indicating that class switching of Ig occurs with anti-NeuGc specificity.

Anti-NeuGc Abs exhibited cytotoxicity against NeuGc-expressing cells

We examined the Ab-dependent cytotoxicity of sera obtained from $CMAH^{-/-}$ mice or healthy human volunteers having anti-NeuGc Abs against thymocytes obtained from $CMAH^{+/+}$ or $CMAH^{-/-}$ mice. Lysis of NeuGc-expressing thymocytes was significantly higher than that of thymocytes lacking NeuGc in both experiments (Fig. 3*A*, 3*B*), indicating that anti-NeuGc Abs show obvious cytotoxicity against NeuGc-expressing cells in vitro. The cytotoxic activity of anti-NeuGc Abs was also determined in vivo. In the FCM analysis, the surviving splenocyte inocula were clearly detected as CFSE-labeled cells in the spleen of control $CMAH^{+/+}$ recipients. In contrast, injected splenocytes were completely absent in the spleen of $CMAH^{-/-}$ recipients at this time point (Fig. 3*C*, 3*D*), indicating that anti-NeuGc Abs eliminated NeuGc-expressing cells in vivo.

CMAH$^{-/-}$ *mice rejected the NeuGc-expressing islets transplanted from syngeneic* CMAH$^{+/+}$ *mice*

Immunohistochemical analysis revealed NeuGc expression on the islets of $CMAH^{+/+}$ and even $GalT^{-/-}$ mice (Fig. 1*A*), but did not reveal any Gal epitopes on the islets of either $CMAH^{+/+}$ or $CMAH^{-/-}$ mice (data not shown). When the islets of $CMAH^{+/+}$ or $CMAH^{-/-}$ mice were incubated with $CMAH^{-/-}$ sera containing anti-NeuGc Abs, the deposition of both IgM and IgG Abs was observed only in the islets obtained from $CMAH^{+/+}$ mice (Fig. 4). Islets obtained from WT $CMAH^{+/+}$ or $GalT^{+/+}$ mice

were transplanted under the kidney capsules of streptozotocin-induced diabetic $CMAH^{+/+}$ mice, $CMAH^{-/-}$ mice having anti-NeuGc Abs, and $GalT^{-/-}$ mice having anti-Gal Abs. Almost all of the $CMAH^{+/+}$ and $GalT^{-/-}$ mice that received 200 iEQs became normoglycemic 1 d after the transplantation (Fig. 5*A*). In contrast, all the $CMAH^{-/-}$ mice that received the same number of syngeneic islets failed to achieve normoglycemia, thus indicating that anti-NeuGc Abs have an inhibitory effect on the engraftment of $CMAH^{+/+}$ islets (Fig. 5*A*, 5B). In an attempt to overcome this inhibitory effect, a larger number of islets was transplanted into diabetic $CMAH^{-/-}$ mice. Normoglycemia was achieved in the $CMAH^{-/-}$ mice that received 500 iEQs (Fig. 5*C*), indicating that a high dose of islets can overcome the anti-NeuGc Ab-mediated resistance to islet engraftment.

In addition, when compared with the control $CMAH^{+/+}$ recipient mice 3 d after islet transplantation, there was a significant decrease in insulin-producing viable β cells in the islet grafts of $CMAH^{-/-}$ recipient mice (Fig. 6). Thus, NeuGc epitopes on the islets were targeted by the corresponding Abs in $CMAH^{-/-}$ recipients (i.e., $CMAH^{-/-}$ mice rejected the NeuGc-expressing islets transplanted from $CMAH^{+/+}$ mice).

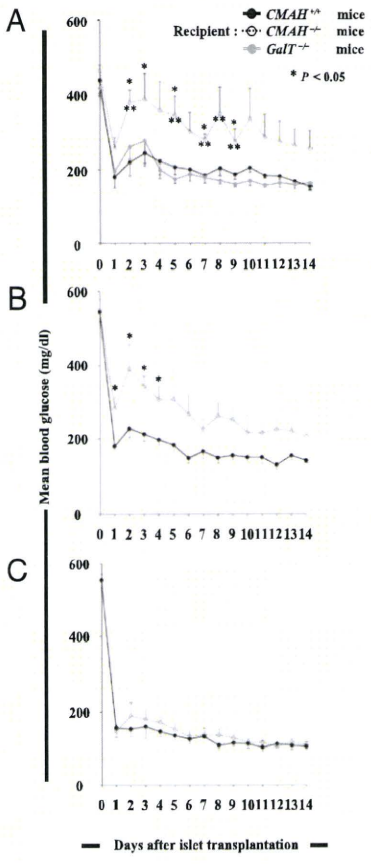

FIGURE 5. Glycemic responses to islet transplantation. Streptozotocin-induced diabetic $CMAH^{+/+}$ mice, $CMAH^{-/-}$ mice having anti-NeuGc Abs, or $GalT^{-/-}$ mice having anti-Gal Abs received kidney capsule transplants of 200 (*A*), 350 (*B*), or 500 iEQs (*C*) obtained from $CMAH^{+/+}$ mice [$n = 5$ for each mouse strain receiving 200 or 350 iEQs (*A*, *B*), and $n = 4$ for each mouse strain receiving 500 iEQs (*C*)]. The blood glucose (mg/dl) measurements of mice are expressed as the mean ± SEM. $*p <$ 0.05 (compared with $CMAH^{+/+}$ recipients); $**p < 0.05$ (compared with $GalT^{-/-}$ recipients).

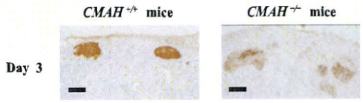

FIGURE 6. Immunohistochemical staining for insulin in the islet grafts. The islet grafts were harvested at day 3 posttransplantation from control $CMAH^{+/+}$ or $CMAH^{-/-}$ recipient mice receiving 200 iEQs from $CMAH^{+/+}$ mice ($n = 3$, each mouse strain). When compared with the control $CMAH^{+/+}$ recipient mice, the representative histological findings show a significant decrease in insulin-producing viable β cells in the islet grafts of $CMAH^{-/-}$ recipient mice. Original magnification ×200. Scale bars, 100 μm.

Binding of NeuGc determinants on the endothelium of vascularized xenograft hearts to the corresponding Abs did not deteriorate their rejection

To examine the immunogenicity of NeuGc epitopes on the endothelium of vascularized organ grafts, we transplanted NeuGc-expressing heart grafts from either syngeneic $CMAH^{+/+}$ B6 mice or xenogeneic neonatal F344 rats into either $CMAH^{-/-}$ mice having anti-NeuGc Abs or control $CMAH^{+/+}$ mice lacking anti-NeuGc Abs. The survival curves of the grafted hearts are shown in Fig. 7. WT B6 hearts survived indefinitely in $CMAH^{-/-}$ mouse recipients (>100 d). In contrast, rat heart xenografts were rejected in $CMAH^{-/-}$ recipients and control $CMAH^{+/+}$ recipients with equal tempo. Even when rabbit complement was injected into these recipient animals to promote complement-dependent cytotoxicity, the tempo of rat heart xenograft rejection in $CMAH^{+/+}$ and $CMAH^{-/-}$ recipients did not differ. Thus, binding of the NeuGc determinants on the endothelium of vascularized xenografts to the corresponding Abs did not accelerate their rejection.

Discussion

In this study, we demonstrated that NeuGc epitopes were absent from the vascular endothelium and other tissues of $CMAH^{-/-}$ mice. These animals, like humans, developed anti-NeuGc Abs, which are normally absent in WT $CMAH^{+/+}$ mice, as a consequence of immunization with NeuGc-expressing cells. They thus provide a model for evaluating the immunogenic property of NeuGc determinants as targets of the corresponding Abs in $CMAH^{+/+}$-to-$CMAH^{-/-}$ transplantation. Previous studies on the transplantation of $GalT^{-/-}$ pig hearts into baboons have revealed that following transplantation, acute humoral xenograft rejection develops, and that this rejection is associated with the presence of

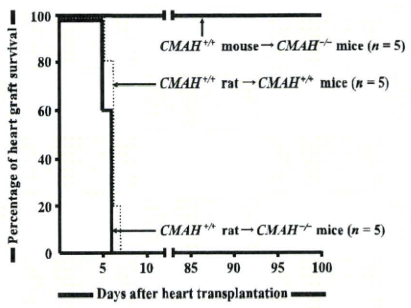

FIGURE 7. The survival curves of grafted hearts. To examine the immunogenicity of NeuGc epitopes in the endothelium of vascularized organ grafts, we transplanted NeuGc-expressing heart grafts from neonatal xenogeneic rats to either $CMAH^{+/+}$ or $CMAH^{-/-}$ mice. Eight weeks before heart transplantation, the recipient mice were i.p. immunized with cells of the NeuGc-expressing porcine endothelial cell line MYP30 to induce anti-NeuGc Abs. We also transplanted syngeneic heart grafts from $CMAH^{+/+}$ to $CMAH^{-/-}$ B6 mice that were immunized with the porcine MYP30 cells. The survival curves of the grafted hearts are shown (each $n = 5$).

preformed or elicited Abs to non-Gal epitopes on $GalT^{-/-}$ pigs (30, 31). However, the non-Gal Abs observed in the $GalT^{-/-}$ pig-to-baboon transplantation model cannot be associated with anti-NeuGc Abs. It is very likely that anti-NeuGc Abs will prove to be important in the clinical application of xenotransplantation, but only after the acute humoral xenograft rejection in pig-to-baboon xenotransplantation is overcome.

To evaluate anti-Gal Abs, $GalT^{-/-}$ mice have been used as a small animal model (24, 26, 32, 33). These mice produce anti-Gal natural Abs (NAbs), similar to humans (24, 32) and $GalT^{-/-}$ pigs (34), although the baseline level of production of anti-Gal Abs in $GalT^{-/-}$ mice is lower than that in humans (35). Because NAbs against Gal are thought to develop as a result of exposure to environmental bacteria that express the Gal determinant (36), the lower levels of anti-Gal NAbs in $GalT^{-/-}$ mice may be due to lower levels of environmental stimulation by the gastrointestinal bacterial flora within the experimental animal facilities (35). In contrast, anti-NeuGc NAbs were undetectable in $CMAH^{-/-}$ mice without stimulation and even upon similar environmental stimulation, suggesting the lower antigenicity of NeuGc epitopes compared with Gal epitopes. Anti-NeuGc Abs were, however, elicited to a certain degree by immunization with NeuGc-expressing syngeneic cells. The production of anti-NeuGc Abs was more pronounced when $CMAH^{-/-}$ mice were immunized with NeuGc-expressing xenogeneic cells (Fig. 2). A similar trend of Ab production against Gal in $GalT^{-/-}$ mice has been observed in previous studies (37, 38). These findings suggest that the production of anti-NeuGc and anti-Gal Abs might be facilitated by the activation of T cells responding to immunogenic xenopeptides on glycoproteins containing NeuGc and Gal epitopes. Such a distinctive contribution of T cells might be relevant to the biased class switching of anti-NeuGc Abs [i.e., IgG1 and IgG3 isotypes were dominantly detected among anti-NeuGc IgGs, resembling the anti-Gal IgG subclasses produced in $GalT^{-/-}$ mice (35)]. Considering the fact that IgM and IgG3 are potent activators of complement (39), this complement-fixing isotype of anti-NeuGc Abs is likely to contribute to humoral rejection. Consistently, we have demonstrated that anti-NeuGc Abs obtained from $CMAH^{-/-}$ mice or healthy human volunteers initiate complement-mediated lysis against $CMAH^{+/+}$ cells in vitro (Fig. 3*A*, 3*B*). In addition, $CMAH^{-/-}$ mice completely rejected NeuGc-expressing splenocytes transplanted from syngeneic $CMAH^{+/+}$ mice (Fig. 3*C*, 3*D*). In that in vivo model, the other dominant isotype of anti-NeuGc IgG in the sera of $CMAH^{-/-}$ mice (i.e., noncomplement-fixing IgG1) might also contribute to the rejection of NeuGc-expressing cells, probably through Ab-dependent cell-mediated cytotoxicity. This assumption is supported by the fact that noncomplement-fixing isotypes of IgG Abs in human sera have the ability to lyse porcine endothelium via Ab-dependent cell-mediated cytotoxicity (40). Further studies are needed to clarify this issue. Nevertheless, the immunogenic property of NeuGc determinants is defined in this study as targets of the corresponding Abs in $CMAH^{+/+}$-to-$CMAH^{-/-}$ cell transplantation.

Islet transplantation is thought to be the most feasible clinical application of pig-to-human xenotransplantation. In a previous study, the expression of NeuGc epitopes on islets from adult or neonatal pigs was clearly detected, and the antigenicity of adult pig islets or neonatal porcine islet-like cell clusters was found to be mainly associated with *N*-linked sugars, including NeuGc epitopes, but not Gal Ags (41–44). These findings led us to investigate the immunogenicity of NeuGc epitopes located on the islets by using a $CMAH^{+/+}$-to-$CMAH^{-/-}$ mouse islet transplantation model. As shown in Figs. 4–6, $CMAH^{-/-}$ mice rejected the NeuGc-expressing islets transplanted from $CMAH^{+/+}$ mice. This result provides further insight into the non-Gal Ab-mediated rejection of porcine islet xenografts and suggests that the genetic manipulation of porcine cells for NeuGc expression could be a novel approach for attenuating non-Gal Ab-mediated islet xenograft rejection. As a further model to investigate xenogeneic setting, we carried out rat-to-$CMAH^{-/-}$ mouse islet transplantation in a separate experiment. However, the rat islet xenografts were rejected in $CMAH^{-/-}$ recipients and control $CMAH^{+/+}$ recipients with equal tempo (Supplemental Fig. 1*A*). This result could be due to the much lower expression of NeuGc epitopes in rat islets than in porcine and mouse islets (Supplemental Fig. 1*B*, 1*C*), indicating that rat-to-$CMAH^{-/-}$ islet transplantation could not be a relevant model to investigate anti-NeuGc Ab-mediated rejection.

In contrast, $CMAH^{-/-}$ mice did not reject vascularized NeuGc-expressing heart grafts, even if exogenous rabbit complement was added (Fig. 7). We have previously described the rejection of $GalT^{+/+}$ mouse or rat hearts by $GalT^{-/-}$ mice and demonstrated this to be a model of HAR, which would occur in pig-to-human/primate xenotransplantation, where anti-Gal Abs and complement mediate HAR (26, 35). The different outcome of $CMAH^{+/+}$ heart grafts in $CMAH^{-/-}$ and $GalT^{-/-}$ mice indicates that the anti-NeuGc Ab-mediated immune response may not be crucially involved in the graft loss in xenogeneic organ transplantation. However, further investigations using organ xenotransplantation models other than the heart should be undertaken to clearly establish whether it is necessary to eliminate NeuGc epitopes because the expression of NeuGc is thought to be dependent on the tissue and developmental stage (28).

Acknowledgments

We thank Dr. Megan Sykes for helpful review of the manuscript, Drs. Kohei Ishiyama, Masayuki Shishida, Toshimitsu Irei, Masahiro Ohira, and Masataka Banshodani for advice and encouragement, Yuka Igarashi, Midori Kiyokawa, and Yuko Ishida for technical assistance, and Dr. Syuji Miyagawa for providing porcine MYP30 cells.

Disclosures

The authors have no financial conflicts of interest.

References

1. Sachs, D. H. 1994. The pig as a xenograft donor. *Pathol. Biol. (Paris)* 42: 217–219.
2. Galili, U., E. A. Rachmilewitz, A. Peleg, and I. Flechner. 1984. A unique natural human IgG antibody with anti-α-galactosyl specificity. *J. Exp. Med.* 160: 1519–1531.
3. Galili, U., B. A. Macher, J. Buehler, and S. B. Shohet. 1985. Human natural anti-α-galactosyl IgG. II. The specific recognition of α(1 → 3)-linked galactose residues. *J. Exp. Med.* 162: 573–582.
4. Ye, Y., F. A. Neethling, M. Niekrasz, E. Koren, S. V. Richards, M. Martin, S. Kosanke, R. Oriol, and D. K. Cooper. 1994. Evidence that intravenously administered α-galactosyl carbohydrates reduce baboon serum cytotoxicity to pig kidney cells (PK15) and transplanted pig hearts. *Transplantation* 58: 330–337.
5. Xu, Y., T. Lorf, T. Sablinski, P. Gianello, M. Bailin, R. Monroy, T. Kozlowski, M. Awwad, D. K. Cooper, and D. H. Sachs. 1998. Removal of anti-porcine natural antibodies from human and nonhuman primate plasma in vitro and in vivo by a Gα1-3Galβ1-4βGlc-X immunoaffinity column. *Transplantation* 65: 172–179.
6. Phelps, C. J., C. Koike, T. D. Vaught, J. Boone, K. D. Wells, S. H. Chen, S. Ball, S. M. Specht, I. A. Polejaeva, J. A. Monahan, et al. 2003. Production of α1,3-galactosyltransferase-deficient pigs. *Science* 299: 411–414.
7. Lai, L., D. Kolber-Simonds, K. W. Park, H. T. Cheong, J. L. Greenstein, G. S. Im, M. Samuel, A. Bonk, A. Rieke, B. N. Day, et al. 2002. Production of α-1,3-galactosyltransferase knockout pigs by nuclear transfer cloning. *Science* 295: 1089–1092.
8. Kuwaki, K., Y. L. Tseng, F. J. Dor, A. Shimizu, S. L. Houser, T. M. Sanderson, C. J. Lancos, D. D. Prabharasuth, J. Cheng, K. Moran, et al. 2005. Heart transplantation in baboons using α1,3-galactosyltransferase gene-knockout pigs as donors: initial experience. *Nat. Med.* 11: 29–31.
9. Yamada, K., K. Yazawa, A. Shimizu, T. Iwanaga, Y. Hisashi, M. Nuhn, P. O'Malley, S. Nobori, P. A. Vagefi, C. Patience, et al. 2005. Marked prolongation of porcine renal xenograft survival in baboons through the use of α1,3-galactosyltransferase

gene-knockout donors and the cotransplantation of vascularized thymic tissue. *Nat. Med.* 11: 32–34.
10. Chen, G., H. Qian, T. Starzl, H. Sun, B. Garcia, X. Wang, Y. Wise, Y. Liu, Y. Xiang, L. Copeman, et al. 2005. Acute rejection is associated with antibodies to non-Gal antigens in baboons using Gal-knockout pig kidneys. *Nat. Med.* 11: 1295–1298.
11. Cooper, D. K. 1998. Xenoantigens and xenoantibodies. *Xenotransplantation* 5: 6–17.
12. Ezzelarab, M., D. Ayares, and D. K. Cooper. 2005. Carbohydrates in xenotransplantation. *Immunol. Cell Biol.* 83: 396–404.
13. Higashi, H., M. Naiki, S. Matuo, and K. Okouchi. 1977. Antigen of "serum sickness" type of heterophile antibodies in human sera: indentification as gangliosides with N-glycolylneuraminic acid. *Biochem. Biophys. Res. Commun.* 79: 388–395.
14. Merrick, J. M., R. Schifferle, K. Zadarlik, K. Kano, and F. Milgrom. 1977. Isolation and partial characterization of the heterophile antigen of infectious mononucleosis from bovine erythrocytes. *J. Supramol. Struct.* 6: 275–290.
15. Merrick, J. M., K. Zadarlik, and F. Milgrom. 1978. Characterization of the Hanganutziu-Deicher (serum-sickness) antigen as gangliosides containing n-glycolylneuraminic acid. *Int. Arch. Allergy Appl. Immunol.* 57: 477–480.
16. Morozumi, K., T. Kobayashi, T. Usami, T. Oikawa, Y. Ohtsuka, M. Kato, O. Takeuchi, K. Koyama, H. Matsuda, I. Yokoyama, and H. Takagi. 1999. Significance of histochemical expression of Hanganutziu-Deicher antigens in pig, baboon and human tissues. *Transplant. Proc.* 31: 942–944.
17. Zhu, A., and R. Hurst. 2002. Anti-N-glycolylneuraminic acid antibodies identified in healthy human serum. *Xenotransplantation* 9: 376–381.
18. Miwa, Y., T. Kobayashi, T. Nagasaka, D. Liu, M. Yu, I. Yokoyama, A. Suzuki, and A. Nakao. 2004. Are N-glycolylneuraminic acid (Hanganutziu-Deicher) antigens important in pig-to-human xenotransplantation? *Xenotransplantation* 11: 247–253.
19. Tangvoranuntakul, P., P. Gagneux, S. Diaz, M. Bardor, N. Varki, A. Varki, and E. Muchmore. 2003. Human uptake and incorporation of an immunogenic nonhuman dietary sialic acid. *Proc. Natl. Acad. Sci. USA* 100: 12045–12050.
20. Varki, A. 2001. Loss of N-glycolylneuraminic acid in humans: Mechanisms, consequences, and implications for hominid evolution. *Am. J. Phys. Anthropol.* (Suppl 33): 54–69.
21. Saethre, M., B. C. Baumann, M. Fung, J. D. Seebach, and T. E. Mollnes. 2007. Characterization of natural human anti-non-gal antibodies and their effect on activation of porcine gal-deficient endothelial cells. *Transplantation* 84: 244–250.
22. Bouhours, D., C. Pourcel, and J. E. Bouhours. 1996. Simultaneous expression by porcine aorta endothelial cells of glycosphingolipids bearing the major epitope for human xenoreactive antibodies (Gal α1-3Gal), blood group H determinant and N-glycolylneuraminic acid. *Glycoconj. J.* 13: 947–953.
23. Naito, Y., H. Takematsu, S. Koyama, S. Miyake, H. Yamamoto, R. Fujinawa, M. Sugai, Y. Okuno, G. Tsujimoto, T. Yamaji, et al. 2007. Germinal center marker GL7 probes activation-dependent repression of N-glycolylneuraminic acid, a sialic acid species involved in the negative modulation of B-cell activation. *Mol. Cell. Biol.* 27: 3008–3022.
24. Thall, A. D., P. Malý, and J. B. Lowe. 1995. Oocyte Galα1,3Gal epitopes implicated in sperm adhesion to the zona pellucida glycoprotein ZP3 are not required for fertilization in the mouse. *J. Biol. Chem.* 270: 21437–21440.
25. Miyagawa, S., R. Shirakura, K. Iwata, S. Nakata, G. Matsumiya, H. Izutani, H. Matsuda, A. Terado, M. Matsumoto, S. Nagasawa, et al. 1994. Effects of transfected complement regulatory proteins, MCP, DAF, and MCP/DAE hybrid, on complement mediated swine endothelial cell lysis. *Transplantation* 58: 834–840.
26. Ohdan, H., Y. G. Yang, A. Shimizu, K. G. Swenson, and M. Sykes. 1999. Mixed chimerism induced without lethal conditioning prevents T cell- and anti-Galα1,3Gal-mediated graft rejection. *J. Clin. Invest.* 104: 281–290.
27. Kobayashi, T., I. Yokoyama, A. Suzuki, M. Abe, S. Hayashi, H. Matsuda, K. Morozumi, M. E. Breimer, L. Rydberg, C. G. Groth, et al. 2000. Lack of antibody production against Hanganutziu-Deicher (H-D) antigens with N-glycolylneuraminic acid in patients with porcine exposure history. *Xenotransplantation* 7: 177–180.
28. Malykh, Y. N., L. Shaw, and R. Schauer. 1998. The role of CMP-N-acetylneuraminic acid hydroxylase in determining the level of N-glycolylneuraminic acid in porcine tissues. *Glycoconj. J.* 15: 885–893.
29. Diswall, M., J. Angström, H. J. Schuurman, F. J. Dor, L. Rydberg, and M. E. Breimer. 2007. Studies on glycolipid antigens in small intestine and pancreas from α1,3-galactosyltransferase knockout miniature swine. *Transplantation* 84: 1348–1356.
30. Hisashi, Y., K. Yamada, K. Kuwaki, Y. L. Tseng, F. J. Dor, S. L. Houser, S. C. Robson, H. J. Schuurman, D. K. Cooper, D. H. Sachs, et al. 2008. Rejection of cardiac xenografts transplanted from α1,3-galactosyltransferase gene-knockout (GalT-KO) pigs to baboons. *Am. J. Transplant.* 8: 2516–2526.
31. Tseng, Y. L., K. Moran, F. J. Dor, T. M. Sanderson, W. Li, C. J. Lancos, H. J. Schuurman, D. H. Sachs, and D. K. Cooper. 2006. Elicited antibodies in baboons exposed to tissues from α1,3-galactosyltransferase gene-knockout pigs. *Transplantation* 81: 1058–1062.
32. Thall, A. D., H. S. Murphy, and J. B. Lowe. 1996. α1,3 Galactosyltransferase-deficient mice produce naturally occurring cytotoxic anti-Gal antibodies. *Transplant. Proc.* 28: 556–557.
33. Yang, Y. G., E. deGoma, H. Ohdan, J. L. Bracy, Y. Xu, J. Iacomini, A. D. Thall, and M. Sykes. 1998. Tolerization of anti-Galα1-3Gal natural antibody-forming B cells by induction of mixed chimerism. *J. Exp. Med.* 187: 1335–1342.
34. Dor, F. J., Y. L. Tseng, J. Cheng, K. Moran, T. M. Sanderson, C. J. Lancos, A. Shimizu, K. Yamada, M. Awwad, D. H. Sachs, et al. 2004. α1,3-Galactosyltransferase gene-knockout miniature swine produce natural cytotoxic anti-Gal antibodies. *Transplantation* 78: 15–20.
35. Ohdan, H., K. G. Swenson, H. Kitamura, Y. G. Yang, and M. Sykes. 2001. Tolerization of Galα1,3Gal-reactive B cells in pre-sensitized α1,3-galactosyltransferase-deficient mice by nonmyeloablative induction of mixed chimerism. *Xenotransplantation* 8: 227–238.
36. Auchincloss, H., Jr., and D. H. Sachs. 1998. Xenogeneic transplantation. *Annu. Rev. Immunol.* 16: 433–470.
37. Ohdan, H., K. G. Swenson, H. S. Kruger Gray, Y. G. Yang, Y. Xu, A. D. Thall, and M. Sykes. 2000. Mac-1-negative B-1b phenotype of natural antibody-producing cells, including those responding to Gal α1,3Gal epitopes in α1,3-galactosyltransferase-deficient mice. *J. Immunol.* 165: 5518–5529.
38. Tanemura, M., D. Yin, A. S. Chong, and U. Galili. 2000. Differential immune responses to α-gal epitopes on xenografts and allografts: implications for accommodation in xenotransplantation. *J. Clin. Invest.* 105: 301–310.
39. Schreiber, J. R., L. J. Cooper, S. Diehn, P. A. Dahlhauser, M. F. Tosi, D. D. Glass, M. Patawaran, and N. S. Greenspan. 1993. Variable region-identical monoclonal antibodies of different IgG subclass directed to *Pseudomonas aeruginosa* lipopolysaccharide O-specific side chain function differently. *J. Infect. Dis.* 167: 221–226.
40. Schaapherder, A. F., M. R. Daha, M. T. te Bulte, F. J. van der Woude, and H. G. Gooszen. 1994. Antibody-dependent cell-mediated cytotoxicity against porcine endothelium induced by a majority of human sera. *Transplantation* 57: 1376–1382.
41. McKenzie, I. F., M. Koulmanda, T. E. Mandel, and M. S. Sandrin. 1998. Pig islet xenografts are susceptible to "anti-pig" but not Galα(1,3)Gal antibody plus complement in Gal o/o mice. *J. Immunol.* 161: 5116–5119.
42. Komoda, H., S. Miyagawa, T. Kubo, E. Kitano, H. Kitamura, T. Omori, T. Ito, H. Matsuda, and R. Shirakura. 2004. A study of the xenoantigenicity of adult pig islets cells. *Xenotransplantation* 11: 237–246.
43. Komoda, H., S. Miyagawa, T. Omori, Y. Takahagi, H. Murakami, T. Shigehisa, T. Ito, H. Matsuda, and R. Shirakura. 2005. Survival of adult islet grafts from transgenic pigs with N-acetylglucosaminyltransferase-III (GnT-III) in cynomolgus monkeys. *Xenotransplantation* 12: 209–216.
44. Omori, T., T. Nishida, H. Komoda, Y. Fumimoto, T. Ito, Y. Sawa, C. Gao, S. Nakatsu, R. Shirakura, and S. Miyagawa. 2006. A study of the xenoantigenicity of neonatal porcine islet-like cell clusters (NPCC) and the efficiency of adenovirus-mediated DAF (CD55) expression. *Xenotransplantation* 13: 455–464.

Surg Endosc (2010) 24:1693–1700
DOI 10.1007/s00464-009-0831-6

Alterations in portal vein blood pH, hepatic functions, and hepatic histology in a porcine carbon dioxide pneumoperitoneum model

Makoto Yoshida · Satoshi Ikeda · Daisuke Sumitani · Yuji Takakura · Masanori Yoshimitsu · Manabu Shimomura · Midori Noma · Masakazu Tokunaga · Masazumi Okajima · Hideki Ohdan

Received: 30 June 2009 / Accepted: 15 November 2009 / Published online: 7 January 2010

Abstract
Background Intra-abdominal high pressure and acidosis by carbon dioxide (CO_2) pneumoperitoneum is known to affect various organ functions. In this study, changes in liver functions and liver histology were investigated during CO_2 pneumoperitoneum in a large animal model.
Methods Fourteen white pigs were anesthetized with intubation and controlled ventilation. The pigs in the pneumoperitoneum group (PG) were exposed to CO_2 pneumoperitoneum at an intra-abdominal pressure of 8 mmHg, and those in the open laparotomy group (OG) were subjected to laparotomy. Hemodynamics were measured and liver function tests were performed in the carotid artery and portal vein, and the liver tissue was histologically examined.
Results The blood pressure, PO_2, PCO_2, and pH in the carotid artery did not significantly differ between the groups. In the PG, blood pressure, PO_2, and PCO_2 in the portal vein were elevated while the pH was low. There were no significant differences in the levels of aminotransferases and lactate between the groups. In the PG, the arterial ketone body ratio (AKBR) was low at 90 min and the ICG retention rate was high at 180 min; these values differed significantly compared to those at 0 min. Histological examination revealed liver congestion in the PG and no significant change in the OG. In the PG, the TUNEL assay revealed positive staining in the area with focal lytic changes.
Conclusions CO_2 pneumoperitoneum at an intra-abdominal pressure of 8 mmHg in a porcine model affected liver functions and caused histological changes in the liver. Although it is uncertain whether these alterations observed in the porcine liver occur in humans as well and whether the alterations are reversible after pneumoperitoneum, it may be necessary to pay attention to liver damage during laparoscopic surgery.

Keywords Carbon dioxide pneumoperitoneum · Laparoscopic surgery · Liver function · Liver histology

In the last decade there has been a considerable increase in the use of laparoscopic surgery for the treatment of a number of diseases. Laparoscopic surgery is believed to be a less invasive procedure than conventional open surgery because patients who undergo laparoscopic surgery experience less pain and have short hospital stays and superior cosmesis compared to those who undergo open surgery [1].

During laparoscopic surgery in humans, a pneumoperitoneum is generally created by the continuous insufflation of CO_2 into the peritoneal cavity at an intra-abdominal pressure of 8–12 mmHg. It is now commonly recognized that in animals and humans, a CO_2 pneumoperitoneum that increases intra-abdominal pressure and CO_2 absorption from the peritoneal cavity has several effects not only on inflammatory and immune reactions [2, 3], but also on organ function, including cardiovascular, respiratory, liver,

M. Yoshida · D. Sumitani · Y. Takakura · M. Yoshimitsu · M. Shimomura · M. Noma · M. Tokunaga · H. Ohdan
Department of Surgery, Division of Frontier Medical Science, Programs for Biomedical Research, Graduate School of Biomedical Sciences, Hiroshima University, Hiroshima, Japan

S. Ikeda (✉) · M. Okajima
Department of Endoscopic Surgery and Surgical Science, Graduate School of Biomedical Sciences, Hiroshima University, 1-2-3 Kasumi, Minami-ku, Hiroshima 734-8551, Japan
e-mail: sikeda@hiroshima-u.ac.jp

and renal function [4–6]. The mechanisms underlying the functional changes in the cardiovascular system during pneumoperitoneum have been studied in detail; however, the mechanisms underlying changes in liver function are still unclear. Several studies have reported that the levels of liver enzymes increase in patients undergoing laparoscopic surgery [7–9]; however, unaltered liver function has been also reported [10, 11]. Furthermore, various studies have reported different changes in the hepatic blood flow during pneumoperitoneum [12–16]. The differences in the duration of pneumoperitoneum and intra-abdominal pressure during pneumoperitoneum between the experimental conditions and clinical settings may result in these different outcomes [10].

Thus, the advantages and disadvantages of laparoscopic surgery with regard to liver function remain controversial in both experimental and clinical studies. In this study we investigated the effect of CO_2 pneumoperitoneum on the functions and histology of the liver in a porcine model.

Materials and methods

Experimental design

This study was carried out in accordance with the guidelines recommended by the Committee of Animal Experimentation, Hiroshima University, and the Committee of Research Facilities for Laboratory Animal Science, Natural Science Center for Basic Research and Development (N-BARD), Hiroshima University. For this study, we used 14 specific-pathogen-free, white, male pigs (mean weight = 35.4 kg; range = 35–36 kg). They were randomly allocated to two equivalent groups: the open laparotomy group (OG) and the pneumoperitoneum group (PG). Each pig was made to fast overnight. The following morning the pigs were premedicated with ketamine (10 mg/kg), desperado (0.1 mg/kg), and atropine (0.05 mg/kg) via the intramuscular route. The animals were then orotracheally intubated and mechanically ventilated, maintaining 100% oxygen inspiration (FiO_2) with a tidal volume of 10–15 ml/kg at the rate of 15 breaths/min. Anesthesia was maintained with isoflurane inhalation. Oxygen saturation was continuously monitored. Ringer's lactate solution was administered intravenously at 100 ml/h by varying the infusion rate, when necessary, through a femoral vein line. The animals were kept in the supine decubitus position throughout the experiment. The right carotid artery was cannulated for the collection of arterial blood samples and for recording the heart rate and arterial blood pressure. A midline abdominal incision of 15 and 25 cm was made for the PG and the OG, respectively. In both groups, a liver tissue biopsy sample was obtained from the right lobe for histological analysis. At the same time, the portal vein was cannulated for obtaining portal vein blood samples and for recording the portal vein pressure. A 12-mm supraumbilical trocar was inserted, and a laser Doppler flowmeter probe was introduced into the peritoneal cavity through the trocar. After the preparation, the midline incision was closed in the PG and a pneumoperitoneum was created by injecting CO_2 and maintained at a pressure of 8 mmHg. In the OG, the laparotomy was kept open during the experiment. On completion of the experiment, the animals were euthanized with an intravenous injection of potassium chloride.

Blood sampling

Serial blood gas samples were obtained during the experiment from an arterial cannula placed in the carotid artery or the portal vein. In the OG, the first blood sample was obtained after the laparotomy and in the PG after the closing of the midline incision but before insufflation of CO_2. Blood sampling was carried out at 15, 30, 45, 60, 90, 120, and 180 min. Blood gas analysis was performed immediately in the operating room. Plasma was obtained by centrifuging the blood samples and was stored at –20°C until analysis. Alanine aminotransferase (ALT) levels, aspartate aminotransferase (AST) levels, and the arterial ketone body ratio (AKBR) were determined by standard methods.

Indocyanine green retention test

Indocyanine green (ICG) (1 mg/kg) was injected into the portal vein 15 min before and 180 min after laparotomy in the OG and 15 min before and 180 min after insufflation of CO_2 in the PG. Blood samples were obtained from the carotid artery before injection of ICG and at 5, 10, and 15 min after the injection. Pharmacokinetic parameters were calculated by using a computer program.

Hemodynamic measurements

The baseline hemodynamic measurements were obtained after laparotomy in the OG and after CO_2 insufflation in the PG. Next, measurements were performed at 15, 30, 45, 60, 90, 120, and 180 min. At each time point, the mean carotid arterial blood pressure and portal vein blood pressure were recorded by calibrated pressure transducers.

Liver blood flow measurement

A laser Doppler flowmeter (ALF21, Advance Company Ltd., Tokyo, Japan) was used for measuring liver tissue

perfusion. The laser Doppler flowmeter uses a fiber-optic-based laser Doppler probe to assess the parenchymal blood flow in the liver tissue. The Doppler shift of the laser beam reflected by the red blood cells is monitored. This represents the transport of blood cells through the microvasculature and is defined as follows: microvascular perfusion (FLOW) = number of blood cells moving in the tissue sampling volume (MASS) × mean velocity of these cells (VELOCITY). We continuously measured the liver blood flow in all the pigs from each group. The probe was introduced into the peritoneal cavity through the 12-mm supraumbilical trocar and was secured on the liver surface with tape. We plotted the liver blood flow at each time point on the basis of the value obtained from baseline measurements performed at 0 min.

Tissue sampling and histological analysis

Biopsy samples were taken from the right lobe of the liver. The first sample was taken immediately after the laparotomy and the second sample at 180 min after the first biopsy. We fixed 5-μm paraffin-embedded sections of liver biopsy samples in 10% buffered formalin and stained these with hematoxylin and eosin. All the specimens were evaluated by two pathologists who were blinded to the sequence of the biopsy specimens.

Evaluation of DNA fragmentation

The terminal dUDP nick-end-labeling (TUNEL) assay was performed on the paraffin sections using an in situ apoptosis detection kit (TaKaRa Biomedicals, Otsu, Japan).

Statistical analysis

All data other than the liver blood flow measurements were reported as the mean ± standard deviation (SD). Statistical comparisons were made among groups using the Kruskal–Wallis analysis, and the Mann–Whitney *U* test with Bonferroni correction was used as the post hoc test of variance. Because the data were not normally distributed, nonparametric statistical analysis was used. Friedman's test was used to compare dependent values within the same group. A p value less than 0.05 was considered significant.

Results

Animal conditions and changes in blood pressure, PO_2, PCO_2, and pH in the carotid artery

The time course of hemodynamic parameters and the findings of the blood gas examination of the carotid artery are shown in Fig. 1. No significant difference was observed

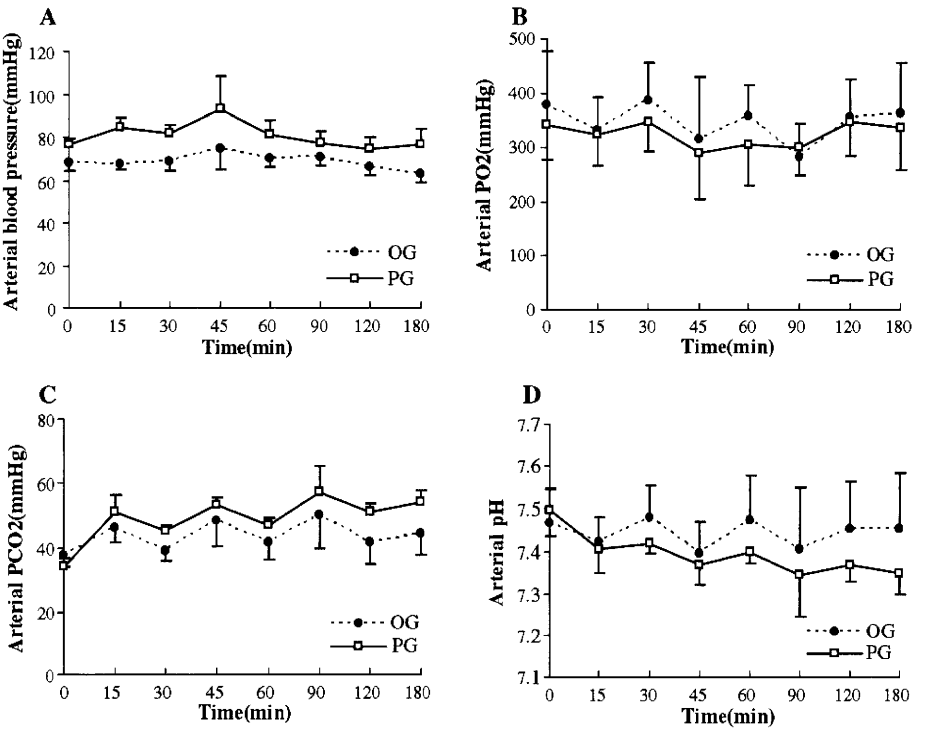

Fig. 1 Time course of the parameters of the carotid artery. **A** Blood pressure. **B** PO_2. **C** PCO_2. **D** pH. *Bars* indicate the mean ± SD. *PG* pneumoperitoneum group, *OG* open group

in the blood pressure, PO_2, PCO_2, and pH between the PG and the OG during the experiments. Furthermore, the heart rate and body temperature did not significantly differ between the two groups (data not shown).

Changes in blood pressure, PO_2, PCO_2, and pH in the portal vein

During the experiments, the blood pressure in the portal vein immediately increased to approximately 15 mmHg in the PG, while it remained constant in the OG (Fig. 2A). Statistical analysis revealed a significant difference in the portal vein blood pressure between the PG and the OG at all time points ($p < 0.01$). The levels of PO_2 and PCO_2 in the portal vein blood were significantly higher in the PG than in the OG at all time points ($p < 0.01$) (Fig. 2B and C, respectively). The pH of the portal vein blood gradually decreased in the PG but not in the OG (Fig. 2D). Furthermore, statistical analysis revealed a significant difference in the pH of the portal vein blood between the PG and the OG at all the time points ($p < 0.01$).

Changes in the levels of hepatic aminotransferases, lactate level, AKBR, and ICG retention test

As shown in Fig. 3A and B, the time course of the AST and ALT levels did not significantly differ between the PG and the OG, while the levels of both AST and ALT were higher in the PG than in the OG at almost all the time points during the experiments. The amount of lactate in the carotid artery remained constant at all the time points in both the PG and the OG (data not shown). In the PG, AKBR decreased at 90 min and significantly differed from that at 0 min ($p < 0.01$) (Fig. 3C). We performed the ICG retention test at 0 and 180 min. The value of the ICG retention test was significantly higher at 180 min than at 0 min in the PG ($p < 0.01$), although this value did not vary significantly in the OG (Fig. 3D).

Liver tissue blood flow

The liver tissue blood flow measured using a laser Doppler flowmeter showed a gradual increase in the PG but remained constant in the OG (Fig. 4), although we could not analyze the statistical differences between the two groups because of the small number of pigs. We have shown the representative data of two pigs in each group because the data of other pigs contained noise.

Histological findings in the liver

Histological examination revealed ballooning and steatosis in the hepatocytes around the central vein and a focal lytic change in the hepatocytes in the PG (Fig. 5B–E). Furthermore, dilatation and congestion of the sinusoid and central vein were observed in the PG (Fig. 5B, C). On the other hand, no obvious change was observed in the OG (Fig. 5A). The assay revealed that TUNEL-positive hepatocytes were present in the region where a focal lytic change was observed in the hepatocytes (Fig. 5F).

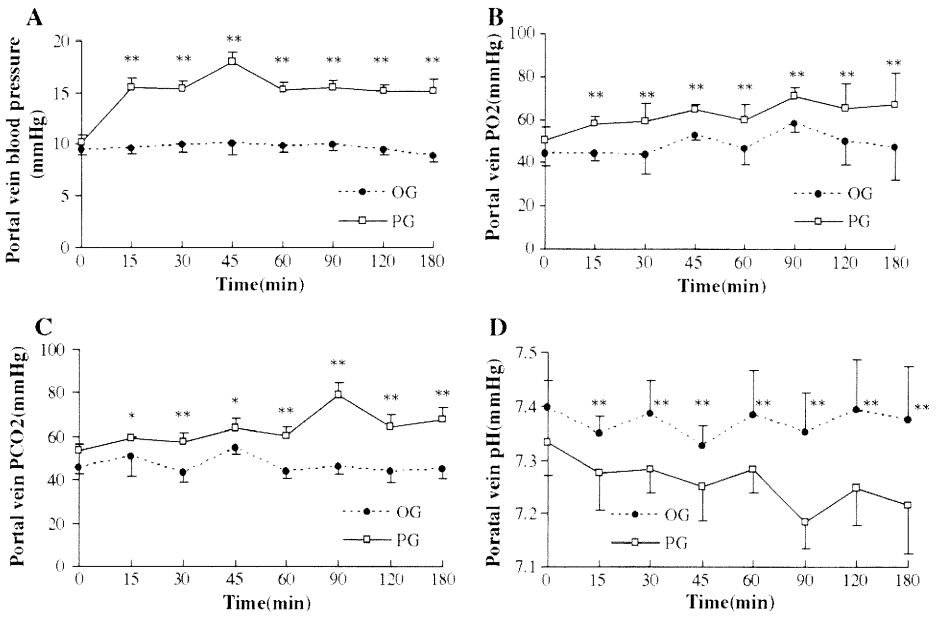

Fig. 2 Time course of the parameters of the portal vein blood. **A** Blood pressure. **B** PO_2. **C** PCO_2. **D** pH. $*p < 0.05$ and $**p < 0.01$ compared to the OG. *Bars* indicate the mean ± SD.
PG pneumoperitoneum group, *OG* open group

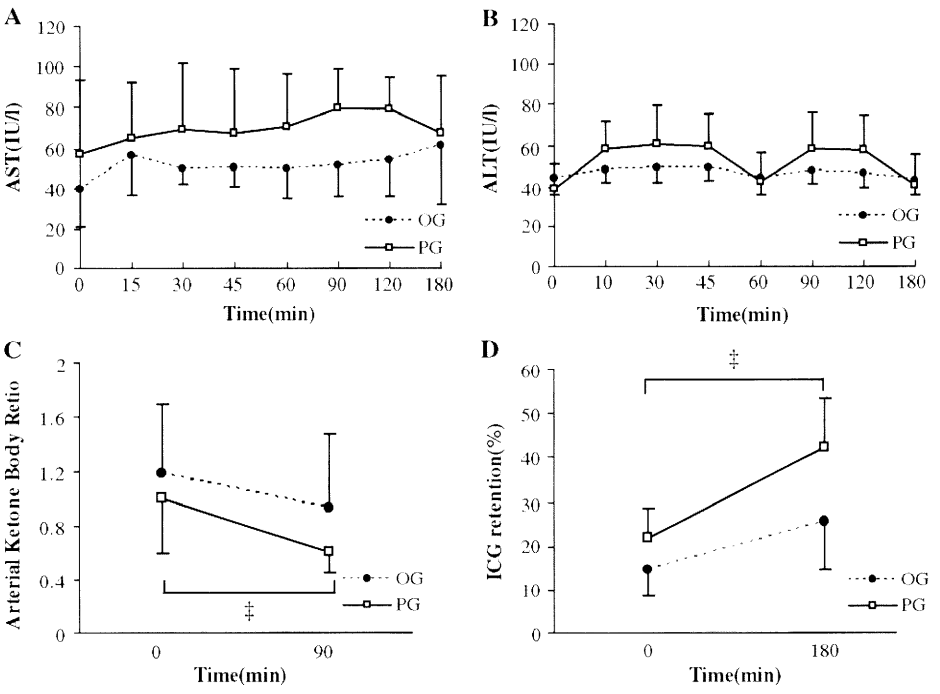

Fig. 3 Time course of AST (**A**), ALT (**B**), changes in AKBR (**C**), and the ICG retention test (**D**). $^{\ddagger}p < 0.01$ compared to the value at 0 min. *Bars* indicate the mean ± SD. *PG* pneumoperitoneum group, *OG* open group

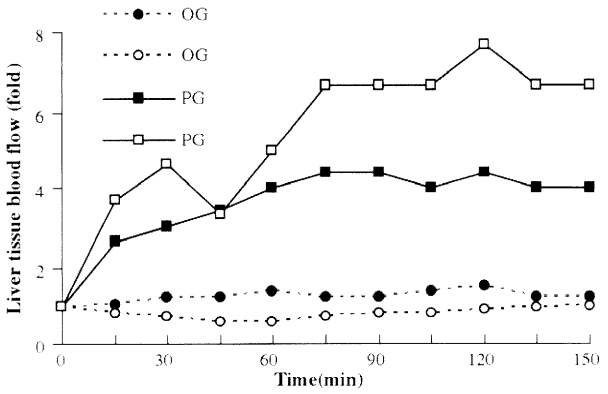

Fig. 4 Time course of the blood flow in the liver tissue. *PG* pneumoperitoneum group, *OG* open group

Discussion

CO_2 insufflation is the most commonly used procedure during laparoscopic surgery. Various studies have shown that a pneumoperitoneum with CO_2 affects the functions of several organs, including the heart, lung, kidney, and liver [4, 6, 17]. In this study we assessed the effects of pneumoperitoneum on liver functions in a porcine pneumoperitoneum model because it is difficult to obtain portal vein blood and liver tissue samples from humans during laparoscopic surgery. We found changes in portal vein acidosis, liver functions, and liver histology during CO_2 pneumoperitoneum.

Hepatic aminotransferases are well-analyzed markers that have been used during and after pneumoperitoneum in humans and animals. Many studies have reported that the levels of aminotransferases remain constant in a low-pressure pneumoperitoneum but increase in a high-pressure pneumoperitoneum [10, 18, 19]. The experiments were performed in pigs under CO_2 pneumoperitoneum at an intra-abdominal pressure of 8 mmHg because at this pressure the general conditions of clinical laparoscopic surgery can be simulated. Moreover, previous studies have reported that low intra-abdominal pressure (7-10 mmHg) had minimal effects on the functions of the heart and other organs [4, 10, 19]. Indeed, there was no significant difference between the two groups with respect to the blood pressure, PO_2, PCO_2, and pH in the carotid artery (Fig. 1). Furthermore, statistical analysis revealed no significant difference in the time course of serum aminotransferase levels between the PG and the OG. These results were consistent with those reported in previous studies. Although statistical analysis revealed no significant difference in the levels of serum aminotransferases between the groups, the results of the present study showed that these levels were higher in the PG than in the OG (Fig. 3). These findings may be consistent with the histological findings, which were lytic changes in a focal area but not in a confluent area of the hepatocytes in the PG and no changes in the hepatocytes of the OG (Fig. 5).

In addition to aminotransferases, we analyzed the lactate levels, AKBR, and ICG retention. There have been few

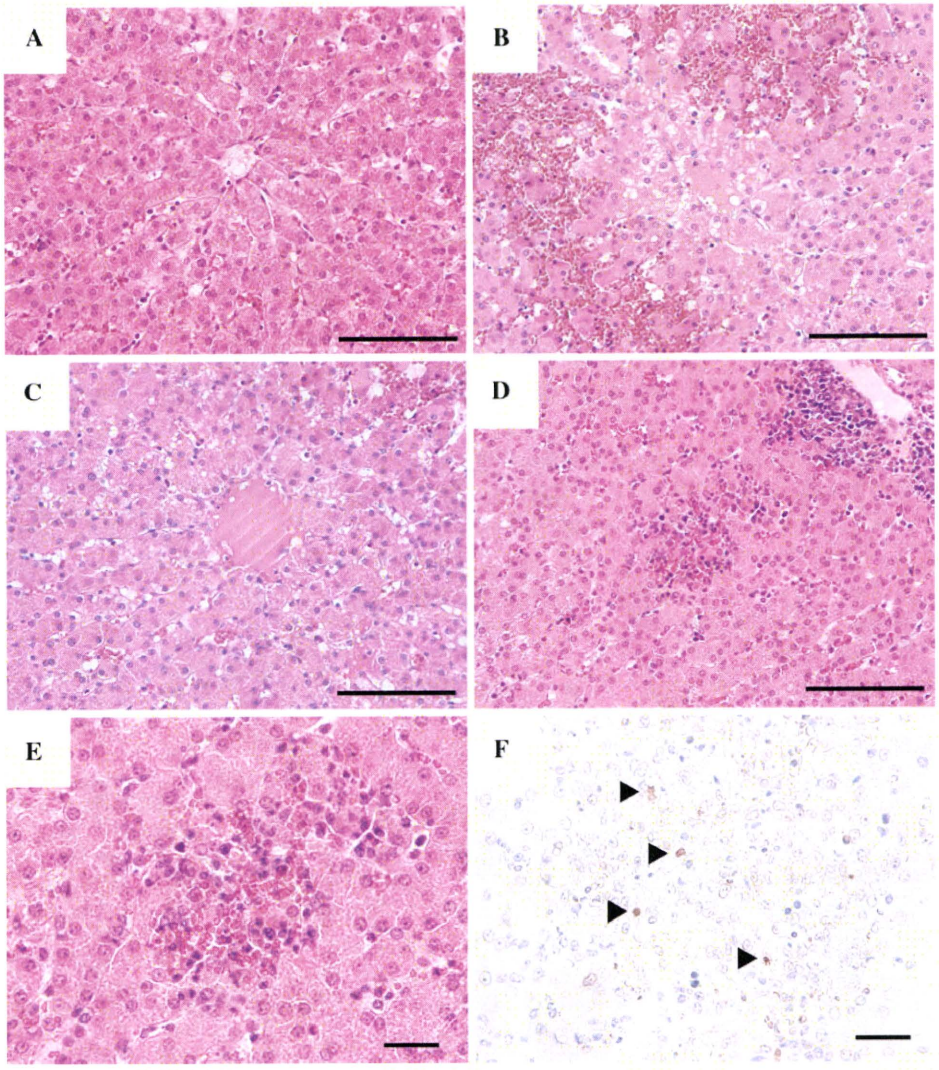

Fig. 5 Histopathological findings of the liver. HE staining of the liver in the **A** OG, **B**–**E** PG, and **F** TUNEL staining in the PG. The *arrows* indicate TUNEL-positive cells. Original magnifications: 100× (scale bar = 200 μm) in **A**, **B**, **C**, and **D**, and 400× (scale bar = 50 μm) in **E** and **F**. *PG* pneumoperitoneum group, *OG* open group

reports describing hepatic functions other than the serum aminotransferase levels during pneumoperitoneum in animals and humans. Lactate is often clinically used as a marker in anaerobic metabolism and is monitored as a marker for liver functions in acute liver failure and major hepatectomy [20]. Under our experimental conditions, the serum level of lactate was not influenced by CO_2 pneumoperitoneum. On the other hand, in the PG, the AKBR, which is a metabolic indicator of liver functions and is considered to be an accurate index of the functional liver reserve [21], was significantly low at 90 min compared to that at 0 min (Fig. 3C). Interestingly, the pH of the portal vein blood was lowest at 90 min in the PG (pH = 7.19 ± 0.05) (Fig. 2D); the time course of the decrease in the AKBR value was similar to that of pH. On the other hand, the PO_2 level in the portal vein was higher in the PG than in the OG at all the time points (Fig. 2B). AKBR, which is the ratio of acetoacetate to 3-hydroxybutyrate in the arterial blood, reflects the mitochondrial redox potential of hepatocytes and the energy state of the liver [22, 23]. It is known that hepatic mitochondrial functions decrease because of not only hypoxia but also acidosis [24]. Interestingly, based on the blood gas examination of the portal vein, we speculated that the decrease in AKBR that was observed in the experiment may be dependent on the decrease in the pH of the portal vein blood and not on hypoxia. In addition, TUNEL-positive hepatocytes, which probably indicate an apoptotic change in the hepatocytes, were observed in the area with focal lytic changes in the PG. Because it has been reported that mitochondrial dysfunction causes apoptosis in hepatocytes [25], it is probable that CO_2 pneumoperitoneum causes apoptosis in hepatocytes by lowering the pH of the portal vein blood, which in turn results in decreased hepatic mitochondrial function. Furthermore, we examined the change in ICG retention during pneumoperitoneum. ICG is an anionic dye and

removed almost exclusively from the liver [26]. In the PG, the rate of ICG retention significantly increased within 180 min; on the other hand, in the OG, the rate of ICG retention did not significantly vary from 0 to 180 min (Fig. 3D). Elimination of ICG from the blood is indicated by the hepatic blood flow, ICG uptake by the hepatocytes, and ICG excretion from the hepatocytes [26]. It remains unclear whether the efficiency of ICG uptake and hepatocyte excretion is influenced by CO_2 pneumoperitoneum. While hepatic mitochondrial dysfunction observed in this experiment may partly influence the functions of hepatocytes, the change in the liver blood flow under pneumoperitoneum may be important for increasing the ICG retention rate.

Several researchers have examined the hemodynamic changes in the liver blood flow under pneumoperitoneum in humans and animals; however, the results remain controversial. Previous studies have described mainly three methods of measuring liver blood flow: (1) measuring the blood flow of the portal vein and hepatic artery by placing the probe directly on the vessels, (2) measuring the hepatic venous flow using transesophageal Doppler echocardiography, and (3) measuring the velocity and number of red blood cells by using a laser Doppler flowmeter on the liver surface. In studies in which the vessel blood flow was measured directly, the blood flow in the portal vein and hepatic artery was found to decrease or remain unchanged under pneumoperitoneum [12–15]. In a previous study that used transesophageal Doppler echocardiography, it was found that the blood flow in the hepatic vein significantly increased during pneumoperitoneum in humans [16]. We estimated the liver blood flow in this experiment by using a laser Doppler flowmeter. This instrument measures the liver blood flow by multiplying the number of blood cells moving in the tissue sampling volume by the mean velocity of these cells (refer to Materials and methods). Although we could show the representative data of the liver blood flow in only a small number of pigs (2 pigs in each group) because of noise interference during measurement, the liver blood flow increased in the PG during CO_2 pneumoperitoneum but showed no apparent change in the OG. The measurements of the liver blood flow and the results of the histological findings, which revealed dilatation of the sinusoid and central vein (containing red blood cells) and a focal lytic change, may indicate liver congestion. It has been reported that CO_2 pneumoperitoneum affects cardiac functions and results in increased pressure in the superior and inferior caval veins in a porcine pneumoperitoneum model (intra-abdominal pressure = 10 mm Hg) [27]. From the findings of the present experiments and the results of previous studies, we speculated that CO_2 pneumoperitoneum causes liver congestion through right ventricular cardiac overload and a decrease in the blood flow of the hepatic artery and portal vein; this results in an increased ICG retention rate and histological changes.

In conclusion, CO_2 pneumoperitoneum at an intra-abdominal pressure of 8 mmHg for 180 min affects liver functions and causes histological changes in the liver in a porcine model. Laparoscopic surgery is currently used not only for cholecystectomy and colectomy but also for hepatectomy for liver donation in living-related liver transplantation and hepatocellular carcinoma. It is not clear whether the alterations observed in the porcine liver occur in humans as well and whether these alterations are reversible after pneumoperitoneum; however, it is probably important to pay attention to liver damage during laparoscopic surgery in patients with liver dysfunction.

Disclosures Makoto Yoshida, Satoshi Ikeda, Daisuke Sumitani, Yuji Takakura, Masanori Yoshimitsu, Manabu Shimomura, Midori Noma, Masakazu Tokunaga, Masazumi Okajima, and Hideki Ohdan have no conflicts of interest or financial ties to disclose.

References

1. Costi R, Denet C, Sarli L, Perniceni T, Roncoroni L, Gayet B (2003) Laparoscopy in the last decade of the millennium: have we really improved? Surg Endosc 17:791–797
2. Vittimberga FJ Jr, Foley DP, Meyers WC, Callery MP (1998) Laparoscopic surgery and the systemic immune response. Ann Surg 227:326–334
3. Gupta A, Watson DI (2001) Effect of laparoscopy on immune function. Br J Surg 88:1296–1306
4. Safran DB, Orlando R 3rd (1994) Physiologic effects of pneumoperitoneum. Am J Surg 167:281–286
5. Henny CP, Hofland J (2005) Laparoscopic surgery: pitfalls due to anesthesia, positioning, and pneumoperitoneum. Surg Endosc 19:1163–1171
6. Demyttenaere S, Feldman LS, Fried GM (2007) Effect of pneumoperitoneum on renal perfusion and function: a systematic review. Surg Endosc 21:152–160
7. Halevy A, Gold-Deutch R, Negri M, Lin G, Shlamkovich N, Evans S, Cotariu D, Scapa E, Bahar M, Sackier JM (1994) Are elevated liver enzymes and bilirubin levels significant after laparoscopic cholecystectomy in the absence of bile duct injury? Ann Surg 219:362–364
8. Morino M, Giraudo G, Festa V (1998) Alterations in hepatic function during laparoscopic surgery. An experimental clinical study. Surg Endosc 12:968–972
9. Saber AA, Laraja RD, Nalbandian HI, Pablos-Mendez A, Hanna K (2000) Changes in liver function tests after laparoscopic cholecystectomy: not so rare, not always ominous. Am Surg 66:699–702
10. Hasukic S (2005) Postoperative changes in liver function tests: randomized comparison of low- and high-pressure laparoscopic cholecystectomy. Surg Endosc 19:1451–1455
11. Bickel A, Weiar A, Eitan A (2008) Evaluation of liver enzymes following elective laparoscopic cholecystectomy: are they really elevated? J Gastrointest Surg 12:1418–1421
12. Klopfenstein CE, Morel DR, Clergue F, Pastor CM (1998) Effects of abdominal CO_2 insufflation and changes of position on hepatic blood flow in anesthetized pigs. Am J Physiol 275:900–905